tion in a family in which all other affected individuals carried the change, a finding confirmed by two independent examiners. This patient showed clinical features that did not differ significantly from the other affected members in her family. At present, it is unclear whether she may be a phenocopy or whether the real pathogenic mutation may exist in other regions within the shared haplotype between *TTCC01* and *Q9H7K4*. Careful observation of her clinical course and more comprehensive genetic analyses of her family are needed. The pathological consequence of the −16C > T substitution in the *puratrophin-1* gene should be further investigated.

In conclusion, we have found that the −16C > T substitution in the 5′ UTR of *puratrophin-1* was very prevalent in ADCA families in Nagano, where the frequency of 16q22-linked ADCA is much higher than that of SCA6, DRPLA, and SCA3/MJD, the most common subtypes in Japan. An accumulation of 16q22-linked ADCA families may be the main reason for the high incidence of SCD in Nagano. Further studies are needed to elucidate the clinical details and molecular pathogenesis of 16q22-linked ADCA.

Acknowledgements We express gratitude to the patients, their families, and clinicians for participating in this study. This work was supported by a grant from the Research Committee of Ataxic Disease, Research on Specific Disease, the Ministry of Health, Labour, and Welfare of Japan.

References

Banfi S, Servadio A, Chung MY, Kwiatkowski TJ Jr, McCall AE, Duvick LA, Shen Y, Roth EJ, Orr HT, Zoghbi HY (1994) Identification and characterization of the gene causing type 1 spinocerebellar ataxia. Nat Genet 7:513–520

Chen DH, Brkanac Z, Verlinde CL, Tan XJ, Bylenok L, Nochlin D, Matsushita M, Lipe H, Wolff J, Fernandez M, Cimino PJ, Bird TD, Raskind WH (2003) Missense mutations in the regulatory domain of PKC gamma: a new mechanism for dominant nonepisodic cerebellar ataxia. Am J Hum Genet 72:839–849

David G, Abbas N, Stevanin G, Durr A, Yvert G, Cancel G, Weber C, Imbert G, Saudou F, Antoniou E, Drabkin H, Gemmill R, Giunti P, Benomar A, Wood N, Ruberg M, Agid Y, Mandel JL, Brice A (1997) Cloning of the SCA7 gene reveals a highly unstable CAG repeat expansion. Nat Genet 17:65–70

Fujigasaki H, Martin JJ, De Deyn PP, Camuzat A, Deffond D, Stevanin G, Dermaut B, Van Broeckhoven C, Durr A, Brice A (2001) CAG repeat expansion in the TATA box-binding protein gene causes autosomal dominant cerebellar ataxia. Brain 124:1939–1947

Harding AE (1993) Clinical features and classification of inherited ataxias. Adv Neurol 61:1–14

Hirano R, Takashima H, Okubo R, Tajima K, Okamoto Y, Ishida S, Tsuruta K, Arisato T, Arata H, Nakagawa M, Osame M, Arimura K (2004) Fine mapping of 16q-linked autosomal dominant cerebellar ataxia type III in Japanese families. Neurogenetics 5:215–221

Holmes SE, O'Hearn EE, McInnis MG, Gorelick-Feldman DA, Kleiderlein JJ, Callahan C, Kwak NG, Ingersoll-Ashworth RG, Sherr M, Sumner AJ, Sharp AH, Ananth U, Seltzer WK, Boss MA, Vieria-Saecker AM, Epplen JT, Riess O, Ross CA, Margolis RL (1999) Expansion of a novel CAG trinucleotide repeat in the 5′ region of PPP2R2B is associated with SCA12. Nat Genet 23:391–392

Imbert G, Saudou F, Yvert G, Devys D, Trottier Y, Garnier JM, Weber C, Mandel JL, Cancel G, Abbas N, Durr A, Didierjean O, Stevanin G, Agid Y, Brice A (1996) Cloning of the gene for spinocerebellar ataxia 2 reveals a locus with high sensitivity to expanded CAG/glutamine repeats. Nat Genet 14:285–291

Ishikawa K, Toru S, Tsunemi T, Li M, Kobayashi K, Yokota T, Amino T et al (2005) An autosomal dominant cerebellar ataxia linked to chromosome 16q22.1 is associated with a single-nucleotide substitution in the 5′ untranslated region of the gene encoding a protein with spectrin repeat and rho guanine-nucleotide exchange-factor domains. Am J Hum Genet 77:280–296

Kawaguchi Y, Okamoto T, Taniwaki M, Aizawa M, Inoue M, Katayama S, Kawakami H, Nakamura S, Nishimura M, Akiguchi I (1994) CAG expansions in a novel gene for Machado-Joseph disease at chromosome 14q32.1. Nat Genet 8:221–228

Koide R, Kobayashi S, Shimohata T, Ikeuchi T, Maruyama M, Saito M, Yamada M, Takahashi H, Tsuji S (1999) A neurological disease caused by an expanded CAG trinucleotide repeat in the TATA-binding protein gene: a new polyglutamine disease? Hum Mol Genet 8:2047–2053

Koob MD, Moseley ML, Schut LJ, Benzow KA, Bird TD, Day JW, Ranum LP (1999) An untranslated CTG expansion causes a novel form of spinocerebellar ataxia (SCA8). Nat Genet 21:379–384

Li M, Ishikawa K, Toru S, Tomimitsu H, Takashima M, Goto J, Takiyama Y, Sasaki H, Imoto I, Inazawa J, Toda T, Kanazawa I, Mizusawa H (2003) Physical map and haplotype analysis of 16q-linked autosomal dominant cerebellar ataxia (ADCA) type III in Japan. J Hum Genet 48:111–118

Margolis RL (2003) Dominant spinocerebellar ataxias: a molecular approach to classification, diagnosis, pathogenesis and the future. Expert Rev Mol Diagn 3:715–732

Maruyama H, Izumi Y, Morino H, Oda M, Toji H, Nakamura S, Kawakami H (2002) Difference in disease-free survival curve and regional distribution according to subtype of spinocerebellar ataxia: a study of 1,286 Japanese patients. Am J Med Genet 114:578–583

Matsuura T, Yamagata T, Burgess DL, Rasmussen A, Grewal RP, Watase K, Khajavi M, McCall AE, Davis CF, Zu L, Achari M, Pulst SM, Alonso E, Noebels JL, Nelson DL, Zoghbi HY, Ashizawa T (2000) Large expansion of the ATTCT pentanucleotide repeat in spinocerebellar ataxia type 10. Nat Genet 26:191–194

Nagafuchi S, Yanagisawa H, Ohsaki E, Shirayama T, Tadokoro K, Inoue T, Yamada M (1994) Structure and expression of the gene responsible for the triplet repeat disorder, dentatorubral and pallidoluysian atrophy (DRPLA). Nat Genet 8:177–182

Nagaoka U, Takashima M, Ishikawa K, Yoshizawa K, Yoshizawa T, Ishikawa M, Yamawaki T, Shoji S, Mizusawa H (2000) A gene on SCA4 locus causes dominantly inherited pure cerebellar ataxia. Neurology 54:1971–1975

Nakamura K, Jeong SY, Uchihara T, Anno M, Nagashima K, Nagashima T, Ikeda S, Tsuji S, Kanazawa I (2001) SCA17, a novel autosomal dominant cerebellar ataxia caused by an expanded polyglutamine in TATA-binding protein. Hum Mol Genet 10:1441–1448

Pulst SM, Nechiporuk A, Nechiporuk T, Gispert S, Chen XN, Lopes-Cendes I, Pearlman S, Starkman S, Orozco-Diaz G, Lunkes A, DeJong P, Rouleau GA, Auburger G, Korenberg JR, Figueroa C, Sahba S (1996) Moderate expansion of a normally biallelic trinucleotide repeat in spinocerebellar ataxia type 2. Nat Genet 14:269–276

Sanpei K, Takano H, Igarashi S, Sato T, Oyake M, Sasaki H, Wakisaka A, Tashiro K, Ishida Y, Ikeuchi T, Koide R, Saito M, Sato A, Tanaka T, Hanyu S, Takiyama Y, Nishizawa M, Shimizu N, Nomura Y, Segawa M, Iwabuchi K, Eguchi I, Tanaka H, Takahashi H, Tsuji S (1996) Identification of the spinocerebellar ataxia type 2 gene using a direct identification of repeat expansion and cloning technique, DIRECT. Nat Genet 14:277–284

Sasaki H, Yabe I, Tashiro K (2003) The hereditary spinocerebellar ataxias in Japan. Cytogenet Genome Res 100:198–205

Schols L, Bauer P, Schmidt T, Schulte T, Riess O (2004) Autosomal dominant cerebellar ataxias: clinical features, genetics, and pathogenesis. Lancet Neurol 3:291–304

Shimizu Y, Yoshida K, Okano T, Ohara S, Hashimoto T, Fukushima Y, Ikeda S (2004) Regional features of autosomal-dominant cerebellar ataxia in Nagano: clinical and molecular genetic analysis of 86 families. J Hum Genet 49:610–616

Takashima M, Ishikawa K, Nagaoka U, Shoji S, Mizusawa H (2001) A linkage disequilibrium at the candidate gene locus for 16q-linked autosomal dominant cerebellar ataxia type III in Japan. J Hum Genet 46:167–171

Van Swieten JC, Brusse E, de Graaf BM, Krieger E, van de Graaf R, de Koning I, Maat-Kievit A, Leegwater P, Dooijes D, Oostra BA, Heutink P (2003) A mutation in the fibroblast growth factor 14 gene is associated with autosomal dominant cerebellar ataxia [corrected]. Am J Hum Genet 72:191–199

Zhuchenko O, Bailey J, Bonnen P, Ashizawa T, Stockton DW, Amos C, Dobyns WB, Subramony SH, Zoghbi HY, Lee CC (1997) Autosomal dominant cerebellar ataxia (SCA6) associated with small polyglutamine expansions in the alpha 1A-voltage-dependent calcium channel. Nat Genet 15:62–69

J Hum Genet (2006) 51:412–417
DOI 10.1007/s10038-006-0376-7

ORIGINAL ARTICLE

Shoko Miura · Kiyonori Miura · Hideaki Masuzaki
Noriko Miyake · Koh-ichiro Yoshiura
Nadiya Sosonkina · Naoki Harada
Osamu Shimokawa · Daisuke Nakayama
Shuichiro Yoshimura · Naomichi Matsumoto
Norio Niikawa · Tadayuki Ishimaru

Microarray comparative genomic hybridization (CGH)-based prenatal diagnosis for chromosome abnormalities using cell-free fetal DNA in amniotic fluid

Received: 9 November 2005 / Accepted: 7 January 2006 / Published online: 19 April 2006

Abstract Cell-free fetal DNA (cffDNA) in the supernatant of amniotic fluid, which is usually discarded, can be used as a sample for prenatal diagnosis. For rapid prenatal diagnosis of frequent chromosome abnormalities, for example trisomies 13, 18, and 21, and monosomy X, using cffDNA, we have developed a targeted microarray-based comparative genomic hybridization (CGH) panel on which BAC clones from chromosomes 13, 18, 21, X, and Y were spotted. Microarray-CGH analysis was performed for a total of 13 fetuses with congenital anomalies using cffDNA from their uncultured amniotic fluid. Microarray CGH with cffDNA led to successful molecular karyotyping for 12 of 13 fetuses within 5 days. Karyotypes of the 12 fetuses (one case of trisomy 13, two of trisomy 18, two of trisomy 21, one of monosomy X, and six of normal karyotype) were later confirmed by conventional chromosome analysis using cultured amniocytes. The one fetus whose molecular-karyotype was indicated as normal by microarray CGH actually had a balanced translocation, 45,XY,-der(14;21)(q10;q10). The results indicated that microarray CGH with cffDNA is a useful rapid prenatal diagnostic method at late gestation for chromosome abnormalities with copy-number changes, especially when combined with conventional karyotyping of cultured amniocytes.

Keywords Rapid prenatal diagnosis · Microarray-comparative genomic hybridization · Cell-free DNA · Uncultured amniotic fluid · Chromosome abnormality

S. Miura · K. Miura (✉) · H. Masuzaki · D. Nakayama
S. Yoshimura · T. Ishimaru
Department of Obstetrics and Gynecology,
Nagasaki University Graduate School of Biomedical Sciences,
1-7-1 Sakamoto, Nagasaki 852-8501, Japan
E-mail: kiyonori@net.nagasaki-u.ac.jp
Tel.: +81-95-8497363
Fax: +81-95-8497365

S. Miura · N. Miyake · K. Yoshiura · O. Shimokawa · N. Niikawa
Department of Human Genetics, Nagasaki University Graduate School of Biomedical Sciences, Nagasaki, Japan

N. Miyake
Department of Pediatrics, Nagasaki University Graduate School of Biomedical Sciences, Nagasaki, Japan

N. Sosonkina
The Research Institute of Personalized Health Sciences, Health Sciences University of Hokkaido, Hokkaido, Japan

N. Harada · O. Shimokawa
Kyushu Medical Science, Nagasaki, Japan

N. Matsumoto
Department of Human Genetics, Yokohama City University Graduate School of Medicine, Yokohama, Japan

N. Matsumoto · N. Niikawa
SORST, Japan Science and Technology Agency (JST), Kawaguchi, Japan

Present address: T. Ishimaru
Department of Obstetrics and Gynecology, Sasebo Chuo Hospital, Nagasaki, Japan

Introduction

Karyotyping of cultured fetal cells is the standard method for prenatal diagnosis of chromosomal abnormalities. It usually requires 10–14 days to receive a result, however, and may have some problems, e.g. occasional failure of cell culture, wrong karyotype because of artifacts during cell culture, and psuedomosaicism associated with maternal-cell contamination. The recently developed microarray-based comparative genomic hybridization (microarray CGH) does not

require dividing cells and enables rapid, automated, high-throughput screening of chromosome abnormalities (Pollack et al. 1999). In this system, DNA from bacteria-derived artificial chromosome (BAC) that had been precisely mapped to regions in the human genome was amplified by the degenerated oligonucleotide primed (DOP)-PCR method and used as target DNA on the microarray (Telenius et al. 1992). Consequently, microarray CGH made rapid whole-chromosome analysis possible in a single experiment, compared with thousands of experiments using independent fluorescence in-situ hybridization (FISH) (Lapierre et al. 2000; Oostlander et al. 2004; Lau and Leung 2005).

Cell-free fetal DNA (cffDNA) in amniotic fluid obtained by amniocentesis is usually ignored and discarded; it is, however, becoming an attractive sample for prenatal diagnosis (Bianchi 2000; Bianchi and Lo 2001; Watanagara and Bianchi 2004; Hahn et al. 2005; Lo 2005). A recent report pointed out that cffDNA from amniotic fluid is a potential sample for microarray-based diagnosis, because its performance in hybridization is similar to that of cellular DNA (Larrabee et al. 2004). However, its accuracy, reproducibility, analytical and clinical validity, and clinical utility have not been well demonstrated. Little is known about whether microarray CGH with cffDNA is a rapid and effective analytical method for diagnosis of unbalanced chromosomal aberrations, or how to use the method in uncultured amniotic fluid. In clinical medicine, situations often arise which involve pregnancies requiring a rapid prenatal diagnosis for appropriate fetal management, for example those with fetal multiple anomalies detected by ultrasound examination at late gestation (Drummond et al. 2003; Nyberg and Souter 2000; Yang et al. 2005). In this situation, utilization of cffDNA from crude amniotic fluid may make it possible to shorten the testing time for molecular karyotyping. Also, as common chromosomal abnormalities during perinatal care were trisomy 13, 18, and 21, and monosomy X, a targeted microarray based CGH panel of these chromosomes could be efficient.

In this study, we investigated whether targeted microarray-CGH analysis using cffDNA in uncultured amniotic fluid can be used for rapid screening for common chromosomal abnormalities.

Materials and methods

Subjects and DNA preparation

Seven fetuses with congenital anomalies in the 15–17th weeks of gestation and six such fetuses in the 32–34th weeks were included in this study. Fresh amniotic fluid (30 mL) was obtained by transabdominal amniocentesis. Two-thirds of the amniotic fluids were used for 400-band-level G-banding chromosome analysis and the remaining 10 mL were for microarray-CGH assay. The 13 fetuses included one case of trisomy 13, two of trisomy 18, two of trisomy 21, one of monosomy X, one of balanced translocation, three of a normal XY karyotype, and three cases of a normal XX karyotype, all of which were diagnosed by conventional karyotyping of their cultured amniocytes. Study procedures were approved by the Committee for the Ethical Issues on Human Genome and Gene Analysis in Nagasaki University, and written informed consent was obtained from all families.

Fresh amniotic fluid (10 mL) was centrifuged at 350*g* for 10 min, and the supernatant was centrifuged again at 13,500*g* for 20 min to remove any remaining cells (Bianchi et al. 2001). The cffDNA was extracted from the second supernatant using the DNA extraction kit (Qiagen, Hilden, Germany). All samples contained at least 800–1,250 ng cffDNA. The performance of the cffDNA in hybridization to microarrays was similar to that of control DNA obtained from a karyotypically normal male adult.

Degenerate oligonucleotide primed (DOP) PCR

Degenerate oligonucleotide primed-PCR was performed to amplify target clone DNA using three different 5′-aminolabeled PCR primers described elsewhere (Harada et al. 2004). PCR was cycled 30 times at 94°C for 30 s, at linear ramping of 37–72°C over 10 min, and at 72°C for 1 min. Successfully amplified PCR products, usually 0.2–2 kb in size, were used for subsequent experiments. Each 100 μL PCR product obtained by use of the three primers was mixed with the same volume of 4× print buffer (1 mol L^{-1} sodium phosphate/0.001% *N*-lauroyl sarcosine, pH 8.5) and concentrated to a final volume of 30 μL using Microcon 100 (Millipore, Bedford, MA, USA). The products were mixed with DMSO and ddH_2O to a final concentration of 1× print buffer/20% DMSO and were ready for prints.

Microarray CGH

Fifty BAC clones (ten clones each on chromosomes 13, 18, 21, X, and Y) selected from the UCSC genome browser were used as target DNA for microarray (Table 1). Their chromosomal location was confirmed by FISH in our laboratory (Miyake et al. 2006). The target clone DNA amplified by DOP-PCR was spotted in triplicate on to CodeLinkTM activated slides (Amersham Bioscience, Buckinghamshire, UK) using Stampman (Nippon Laser and Electronics Laboratory, Nagoya, Japan) with a center-to-center distance of 1 mm between adjacent spots. The same triplicate-spot panel was prepared in duplicate as blocks A and B on the same slide. The slides were then pretreated, denatured, and stored in a desiccator until use.

The procedure used for microarray-CGH analysis has been described elsewhere (Harada et al. 2004; Miyake et al. 2006). Briefly, the 800 ng digested subject DNA was labeled with Cy3, and control DNA with Cy5

Table 1 Bacterial artificial chromosome clones used as targeted DNA for microarray CGH

BAC clones from chromosomes				
13	18	21	X	Y
RP11-110K18	RP11-1035E2	RP11-89H21	RP11-366M24	RP11-375P13
RP11-454J9	RP11-260F12	RP11-1029C20	RP11-363G10	RP11-155J5
RP11-14A4	RP11-108N23	RP11-37K4	RP11-22D19	RP11-324P23
RP11-1021F7	RP11-472N17	RP11-115H17	RP11-383M2	RP11-71M14
RP11-299D1	RP11-89M10	RP11-357B7	RP11-80K1	RP11-262D1
RP11-394C23	RP11-20H17	RP11-102E10	RP11-238K20	RP11-135H9
RP11-121F24	RP11-160B24	RP11-78B20	RP11-35M23	RP11-236J18
RP11-75E6	RP11-89I22	RP11-114H1	RP11-485H23	RP11-256K9
RP11-90C11	RP11-57F7	RP11-190A24	RP11-1003J5	RP11-185N10
RP11-273L21	RP11-89N1	RP11-135B17		RP11-115H13

(CGH 1). Reverse labeling (patient DNA with Cy5, and control DNA with Cy3) was also performed (CGH 2). *Eco*RI-digested genomic DNA was labeled with Cy5- or Cy3-dCTP by random prime labeling. Differently labeled DNA was combined with hybridization buffer (50% formamide, 10% dextran sulfate, 0.1% Tween 20, 2× SSC, 10 mmol L^{-1} Tris–HCl, pH 7.4). After prehybridization with herring sperm DNA and human CotI DNA using an in situ frame (Eppendorf, Hamburg, Germany) surrounding each block on a slide in a hybridization chamber (Genetix, New Milton, UK), labeled probe mixtures of CGH1 and CGH2 were simultaneously applied to blocks A and B, respectively. Slides were incubated at 37°C for 72 h with gentle shaking (5 rpm), and then washed once with solution A (1× PBS with 0.05% Tween 20), twice with solution B (2× SSC with 50% formamide) at 43°C for 15 min, and finally with solution A at room temperature for 10 min twice, with shaking, at room temperature.

Slides were scanned with GenePix 4000B (Axon Instruments, Union City, CA, USA) and analyzed with GenePix Pro 4.0 software (Axon Instruments). The subject-to-control DNA ratio for the microarray-CGH was calculated from data from a single-slide experiment, using the "ratio of means" formula. Average normalized inter-locus fluorescence ratio (ANILFR) was calculated for each CGH (Mantripragada et al. 2003). On the basis of results from a previous study, the normal ANILFR range was defined as average within ±2SD (Harada et al. 2004).

Results

Microarray CGH with Cy-3 labeled cffDNA from a 46,XX fetus and with Cy-5 labeled male control DNA revealed the high subject-to-control (Cy3-to-Cy-5) ratio for X-chromosome BAC clones and the markedly reduced ratio for Y-chromosome clones (Fig. 1a). The reverse test (Cy-5 labeled subject and Cy-3 labeled control) revealed the opposite hybridization pattern (Fig. 1b). These CGH patterns of the fetus well reflected her two X chromosomes and no Y chromosome. When signal intensities for the X and Y chromosome markers of cffDNA from a 46,XY male fetus were compared with those of the male control DNA, no significant difference was observed (Figs. 1c, d). Likewise, microarray CGH with cffDNA from two fetuses which were confirmed later to have trisomy 18 or trisomy 21 revealed the increased subject-to-control ratio for clones of chromosomes 18 and 21, respectively (data not shown). The CGH with cffDNA from a male fetus with a balanced translocation [45,XY,der(14;21)(q10;q10)mat] revealed no different signal intensity from a karyotypically normal male fetus (Fig. 1e).

We also used the microarray-CGH method for diagnosis of six fetuses with congenital abnormalities that were detected by ultrasound examination at late gestation. A 40-year-old primigravida woman at 33 weeks' gestation was referred to our hospital because of her fetus's intrauterine growth retardation (IUGR), polyhydramnios, ventricular septal defect, and an enlarged cisterna magna. The woman also had a severe threatened premature labor and a tocolytic treatment was started. Decompression by amniocentesis was done at 34 weeks' gestation to prevent premature labor, and targeted microarray CGH was performed with cffDNA from amniotic fluid. Because the subject-to-control ratio was increased only for all clones of chromosome 18, the ratio was normal for other autosomal clones (Fig. 2a), and XX patterns were apparent, the fetus was diagnosed to be a girl with trisomy 18. Her karyotype was later confirmed to be 47,XX,+18 by chromosome analysis in her cultured amniocytes. Likewise, two fetuses were successfully diagnosed by the microarray CGH to have trisomy 13 and trisomy 21, respectively, because their cffDNA revealed increased subject-to-control ratio for clones of chromosomes 13 and 21 (Figs. 2b, c). The cffDNA of another case had a decreased ratio for Y-chromosomal clones only and a normal ratio for X-chromosomal clones (Fig. 2d), compared with the ratios for a normal control male, indicating that the fetus had monosomy X. Karyotypes of all these three cases were confirmed later by chromosome analysis of their amniotic cells. The remaining two fetuses were diagnosed to be karyotypically normal by the targeted microarray-based CGH, the results being concordant with results from subsequent karyotyping (data not shown).

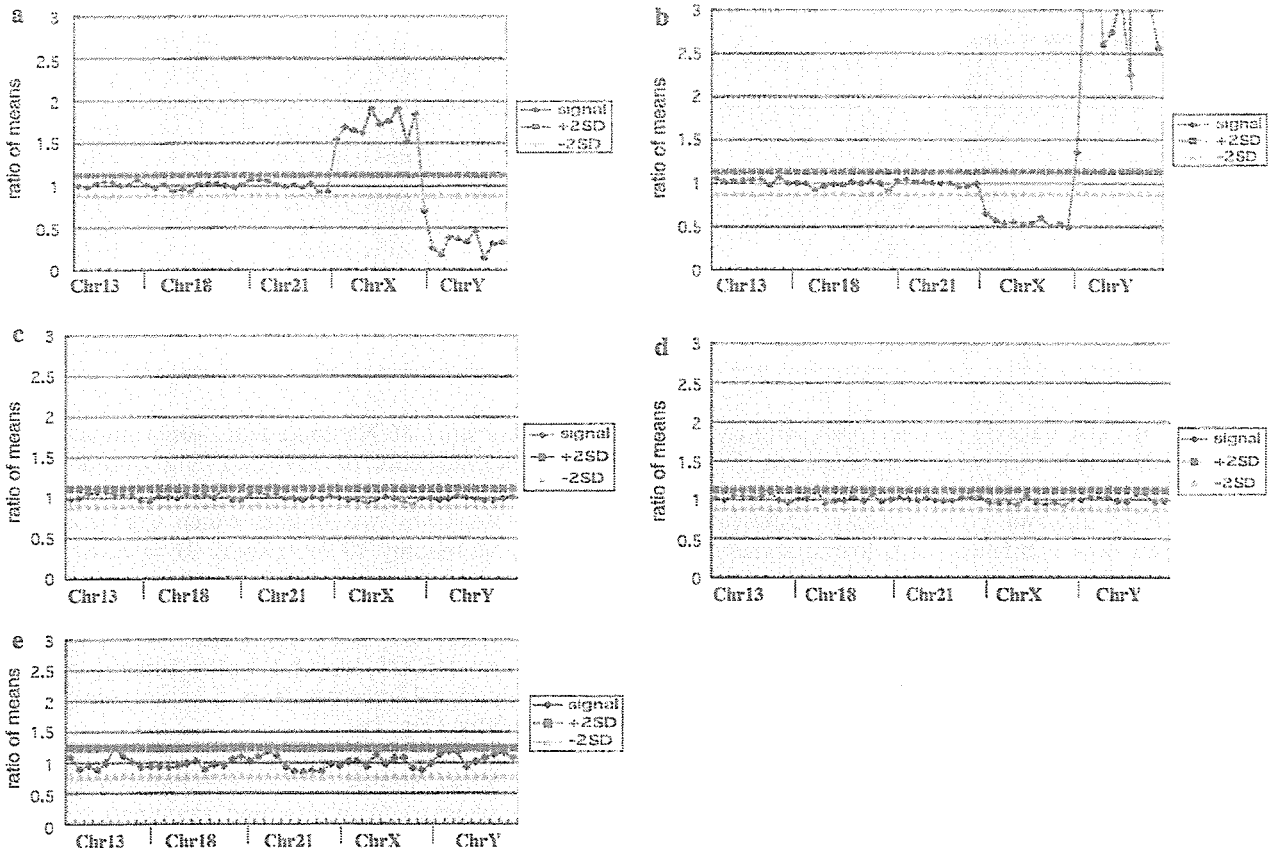

Fig. 1 Microarray-CGH data for female and male cffDNA from uncultured amniotic fluid obtained in the 15–17th gestational weeks, each hybridized separately to arrayed BAC-clones, together with reference DNA from a karyotypically normal adult male. **a** Cy-3-labeled female cffDNA (subject), and Cy-5-labeled male reference DNA (control). **b** Reverse-labeled female cffDNA and male reference DNA. Signal intensity for Y chromosomal clones was infinity, because the normal XX female fetus has no Y chromosome. **c** Cy-3-labeled male cffDNA and Cy-5-labeled male reference DNA. **d** Reverse-labeled male cffDNA and male reference DNA. **e** Cy-3-labeled cffDNA from a male fetus with balanced translocation [45,XY,der(14;21)(q10;q10)mat] and Cy-5-labeled male reference DNA. Vertical axis shows the CGH ratio (Cy-3/Cy-5) value at each locus, and horizontal axis (left to right) 50 BAC clones (ten clones on each chromosome) located to chromosome 13, 18, 21, X, and Y

Discussion

With the development of obstetric ultrasound examinations for a perinatal care, fetal anomalies are often found without the objective of diagnosis (Drummond et al. 2003; Yang et al. 2005). Most such findings do not suggest a specific chromosome region as a target for prenatal diagnosis. In the current microarray-CGH study with cffDNA from uncultured amniotic fluid, we successfully detected abnormal karyotypes in fetuses tested as little as 5 days after amniocentesis. Microarray CGH as a diagnostic tool for chromosome abnormalities has several advantages over conventional and/or FISH-based karyotyping. It enables rapid and comprehensive detection of copy-number changes (deletions or duplications) in the genome in a single experiment (Lapierre at al. 2000; Barrett et al. 2001; Oostlander et al. 2004). In addition, when cffDNA is used as a sample, cell culture is not required. Although inter-phase FISH and quantitative fluorescent PCR (QF-PCR) are also rapid prenatal diagnostic methods, they are applied to limited chromosomal regions at one time. However, BAC-based microarray CGH has some drawbacks. Because its resolving power depends on the number of clones printed and the genomic distance between the clones, a microdeletion or microduplication may be overlooked if the clones printed are less dense. Furthermore, microarray CGH cannot detect balanced rearrangements and diploid/tetraploid mosaics (Amiel et al. 2002; Oostlander et al. 2004). In fact, chromosome abnormalities we have successfully diagnosed were all copy-number changes, and a balanced translocation [45,XY,der(14;21)(q10;q10)] in one fetus could not be diagnosed by this method.

Although the supernatant of the amniotic fluid is usually discarded and ignored as a sample for prenatal chromosomal diagnosis, it contains cffDNA and can be used for genetic testing of the fetus. The reliability, validity, and utility of cffDNA for prenatal diagnosis were very similar to those of DNA isolated from cul-

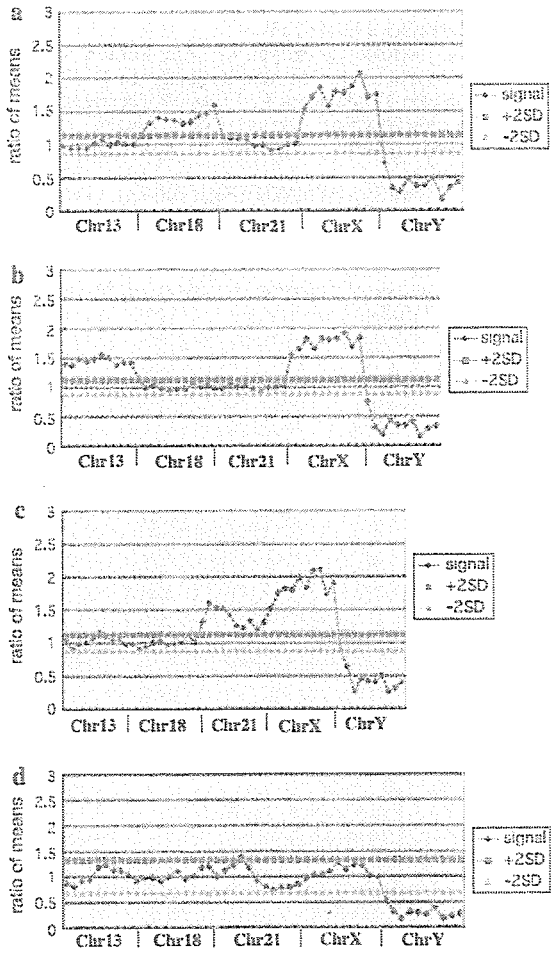

Fig. 2 Microarray-CGH data for cffDNA from uncultured amniotic fluid in the 32–34th gestational weeks of fetuses with numerical chromosome aberrations, each hybridized separately to array clones, together with Cy-5-labeled normal male reference DNA. **a–d** Cy-3-labeled cffDNA from female fetuses with trisomy 18, trisomy 13, trisomy 21, and monosomy X, respectively. The vertical axis shows the CGH ratio (Cy3/Cy5) value for each locus and the horizontal axis shows ten clones each on chromosomes 13, 18, 21, X, and Y

tured amniocytes from the same fetus (Larrabee et al. 2004). Because conventional karyotyping using amniocytes is still invaluable, microarray CGH-based molecular karyotyping with cffDNA should be run in parallel with conventional prenatal karyotyping.

In conclusion, the results of this study indicated that cffDNA in crude amniotic fluid can be used as a sample for microarray-CGH-based prenatal diagnosis of chromosome abnormality. Microarray-CGH with cffDNA enables rapid and comprehensive analysis of copy-number genome changes (Vermeesh et al. 2005). Because of drawbacks of the method, however, it should conducted in combination with conventional karyotyping. The cffDNA also occurs in the maternal circulation. If this technique is applied to cffDNA from the maternal plasma (Masuzaki et al. 2004), it will become a major non-invasive prenatal screening test for fetal chromosome abnormalities.

Acknowledgements We thank Dr Joseph Wagstaff for his help and valuable advice. K.M., H.M., N.M., and N.N. were supported in part by Grants-in-Aid for Scientific Research (Nos. 16591670, 17591748, 16390101, and 13854024, respectively) from the Ministry of Education, Sports, Culture, Science and Technology of Japan, and N.N. was supported by SORST from Japan Science and Technology Agency (JST).

References

Amiel A, Bouaron N, Kidron D, Sharony R, Gaber E, Fejgin MD (2002) CGH in the detection of confined placental mosaicism (CPM) in placentas of abnormal pregnancies. Prenat Diagn 22:752–758

Barrett IJ, Lomax BL, Loukianova T, Tang SS, Lestou VS, Kalousek DK (2001) Comparative genomic hybridization: a new tool for reproductive pathology. Arch Pathol Lab Med 125:81–84

Bianchi DW (2000) Fetal cells in the mother: from genetic diagnosis to diseases associated with fetal cell microchimerism. Eur J Obstet Gynecol Reprod Biol 92:103–108

Bianchi DW, LeShane ES, Cowan JM (2001) Large amounts of cell-free fetal DNA are present in amniotic fluid. Clin Chem 47:1867–1869

Bianchi DW, Lo YM (2001) Fetomaternal cellular and plasma DNA trafficking: the Yin and the Yang. Ann NY Acad Sci 945:119–131

Drummond CL, Gomes DM, Senat MV, Audibert F, Dorion A, Ville Y (2003) Prenat. Diagn 23:1068–1072

Harada N, Hatchwell E, Okamoto N, Tsukahara M, Kurosawa K, Kawame H, Kondoh T, Ohashi H, Tsukino R, Kondoh Y, Shimokawa O, Ida T, Nagai T, Fukushima Y, Yoshiura K, Niikawa N, Matsumoto N (2004) Subtelomere specific microarray based comparative genomic hybridisation: a rapid detection system for cryptic rearrangements in idiopathic mental retardation. J Med Genet 41:130–136

Hahn S, Huppertz B, Holzgreve W (2005) Fetal cells and cell free fetal nucleic acids in maternal blood: new tools to study abnormal placentation? Placenta 26:515–526

Lapierre JM, Cacheux V, Luton D, Collot N, Oury JF, Aurias A, Tachdjian G (2000) Analysis of uncultured amniocytes by comparative genomic hybridization: a prospective prenatal study. Prenat Diagn 20:123–131

Larrabee PB, Johnson KL, Pestova E, Lucas M, Wilber K, LeShane ES, Tantravahi U, Cowan JM, Bianchi DW (2004) Microarray analysis of cell-free fetal DNA in amniotic fluid: a prenatal molecular karyotype. Am J Hum Genet 75:485–491

Lau TK, Leung TN (2005) Genetic screening and diagnosis. Curr Opin Obstet Gynecol 17:163–169

Lo YM (2005) Recent advances in fetal nucleic acids in maternal plasma. J Histochem Cytochem 53:293–296

Mantripragada KK, Buckley PG, Benetkiewicz M, de Bustos C, Hirvela C, Jarbo C, Bruder CEG, Wensman H, Mathiesen T, Nyberg G, Papi L, Collins VP, Ichimura K, Evans G, Dumanski JP (2003) High-resolution profiling of an 11 Mb segment of human chromosome 22 in sporadic schwannoma using array-CGH. Inter J Oncol 22:615–622

Masuzaki H, Miura K, Yoshimura S, Yoshiura K, Ishimaru T (2004) Detection of cell free placental DNA in maternal plasma: direct evidence from three cases of confined placental mosaicism. J Med Genet 41:289–292

Miyake N, Shimokawa O, Harada N, Sosonkina N, Okubo A, Kawara H, Okamoto N, Kurosawa K, Kawame H, Iwakoshi M, Kosho T, Fukushima Y, Makita Y, Yokoyama Y, Yamagata T, Kato M, Hiraki Y, Nomura M, Yoshiura K,

Kishino T, Ohta T, Mizuguchi T, Niikawa N, Matsumoto N (2006) BAC array CGH reveals genomic aberrations in idiopathic mental retardation. Am J Med Genet 140:205–211

Nyberg DA, Souter VL (2000) Sonographic markers of fetal aneuploidy. Clin Perinatol 27:761–789

Oostlander AE, Meijer GA, Ylstra B (2004) Microarray-based comparative genomic hybridization and its applications in human genetics. Clin Genet 66:488–495

Pollack JR, Perou CM, Alizadeh AA, Eisen MB, Pergamenschikov A, Williams CF, Jeffrey SS, Botstein D, Brown PO (1999) Genome-wide analysis of DNA copy-number changes using cDNA microarrays. Nat Genet 23:41–46

Telenius H, Carter NP, Bebb CE, Nordenskjold M, Ponder BA, Tunnacliffe A (1992) Degenerate oligonucleotide-primed PCR: general amplification of target DNA by a single degenerate primer. Genomics 13:718–725

Vermeesch JR, Melotte C, Froyen G, Van Vooren S, Dutta B, Maas N, Vermeulen S, Menten B, Speleman F, De Moor B, Van Hummelen P, Marynen P, Fryns JP, Devriendt K (2005) Molecular karyotyping: array CGH quality criteria for constitutional genetic diagnosis. J Histochem Cytochem 53:413–422

Wataganara T, Bianchi DW (2004) Fetal cell-free nucleic acids in the maternal circulation: new clinical applications. Ann NY Acad Sci 1022:90–99

Yang JH, Chung JH, Shin JS, Choi JS, Ryu HM, Kim MY (2005) Prenatal diagnosis of trisomy 18: report of 30 cases. Prenat Diagn 25:119–122

J Hum Genet (2006) 51:477–479
DOI 10.1007/s10038-006-0388-3

ORIGINAL ARTICLE

Haruka Hamanoue · Nobuko Umezu · Mika Okuda
Naoki Harada · Takako Ohata · Haruya Sakai
Takeshi Mizuguchi · Hiroshi Ishikawa
Tsuneo Takahashi · Kiyonori Miura
Fumiki Hirahara · Naomichi Matsumoto

Complete hydatidiform mole and normal live birth following intracytoplasmic sperm injection

Received: 22 November 2005 / Accepted: 30 January 2006 / Published online: 17 March 2006

Abstract A twin pregnancy with complete hydatidiform mole (HM) and preterm birth of a normal female infant after intracytoplasmic sperm injection (ICSI) conception was experienced. ICSI due to severe oligozoospermia was performed on three ova, and three embryos with confirmed two proneclei (2PN) were subsequently transferred to the uterus. At 7 weeks of gestation, molar pregnancy as well as a viable fetus was recognized. At 33 weeks, the pregnancy was terminated due to preterm labor. Dichorionic pregnancy consisting of a normal fetus and placenta in one chorionic membrane and complete HM in the other was recognized. Cytomolecular analysis indicated that the complete HM genome was derived from duplication of a single sperm, and a normal neonate was from biparental genomes. It should be noted that ICSI can avoid incomplete HM (mostly triploid) due to multi-sperm fertilization but might not be able to avoid complete HM (paternal diploid) although such a risk is very low. This is the second report of this condition and is accompanied by the first well-described molecular analysis.

Keywords Complete mole · ICSI · Normal fetus · Paternal diploid · Twin

H. Hamanoue · T. Ohata · H. Sakai
T. Mizuguchi · N. Matsumoto (✉)
Department of Human Genetics, Graduate School of Medicine, 3-9 Fukuura, Kanazawa-ku, Yokohama 236-0004, Japan
E-mail: naomat@yokohama-cu.ac.jp
Tel.: +81-45-7872604
Fax: +81-45-7865219

H. Hamanoue · N. Umezu · M. Okuda · H. Ishikawa
T. Takahashi · F. Hirahara
Department of Obstetrics and Gynecology and Reproductive Science, Yokohama City University Graduate School of Medicine, Yokohama, Japan

N. Harada
Kyushu Medical Science Nagasaki Laboratory, Nagasaki, Japan

N. Harada · T. Mizuguchi · N. Matsumoto
Solution-Oriented Research for Science and Technology (SORST), JST, Kawaguchi, Japan

K. Miura
Departments of Obstetrics and Gynecology, Nagasaki University Graduate School of Biomedical Sciences, Nagasaki, Japan

Introduction

Hydatidiform mole (HM) with a coexisting fetus is a rare event, with a natural incidence of one in 22,000–100,000 pregnancies (Jones and Lauersen 1975; McDonald and Ruffolo 1983). Two conditions are possible: (1) a twin pregnancy with a complete HM and a normal fetus and placenta; (2) a fetus with a localized placental hydatidiform change (partial HM). Complete HM is diploid in nature, with the genetic material being totally derived from the paternal genome (Kajii and Ohama 1977). Partial HM is mostly triplod in nature, with a combination of diandric (two paternal) haploid sets and one maternal set (Jacobs et al. 1982). The abnormal triploid fetus coexisting with partial HM tends to die in the first trimester, while the fetus coexisting with complete HM does have a chance to survive, as has been previously described (Matsui et al. 2000).

Among recent assisted reproductive technologies (ART), intracytoplasmic sperm injection (ICSI) has the advantage of achieving the successful fertilization of retrieved oocytes irregardless of severe male factors by using micromanipulation techniques, which also enable the direct evaluation of zygotes. In vitro fertilization (IVF) may increase partial HM due to multi-sperm fertilization (Pal et al. 1996), but ICSI may possibly avoid such abnormal conditions as only a single sperm enters an ovum.

We encountered a twin pregnancy with complete HM and a preterm live birth following ICSI. In this article, we report our comprehensive genetic analysis of the products and discuss a possible mechanism by which this condition can occur.

Materials and methods

Case report

A 40-year-old G2P0 woman was referred to our hospital at 16 weeks of gestation (Fig. 1). She had received one cycle of ovarian stimulation and ICSI due to severe oligozoospermia in her husband and subsequent embryo-transfer at a private clinic. ICSI using a single spermatozoon had been performed in each of three metaphase II oocytes. Two pronuclei (2PN) as well as two polar bodies had been recognized in all three embryos the following day. All three embryos – a nine-cell (grade 1–2), a six-cell (grade 1–2), and a three-cell (grade 1–2) – were then transferred into the uterine cavity immediately after a laser-assisted-hatching method. At 6 weeks of gestation, a clinical pregnancy with a heart-beaten fetus (CRL: 7.3 mm) was confirmed. She began to have vaginal bleeding at 7 weeks, and a pregnancy with HM as well as a coexisting fetus was suspected by ultrasound examinations. The pregnancy was continued and the woman was hospitalized at 17 weeks of gestation because of a threatened abortion. At 33 weeks of gestation, her pregnancy was terminated for inevitable preterm labor. A 1544 g (−1.0 SD) female baby was delivered through cesarean section, followed by a total hysterectomy for the prevention of persistent gestational trophoblastic tumor development as the risk of the latter has been reported to be much higher in patients with complete HM and coexisting fetus than in those with single complete HM (Matsui et al. 2000; Ruiz-Casares et al. 2001). The existence of one normal placenta together with the baby in one chorionic sac and apparent molar tissues in the other indicated dichorionic placenta. The molar pregnancy was diagnosed as complete HM macroscopically, and trophoblastic invasion of the myometrium or a malignant tumor of trophoblastic epithelium was not recognized histopathologically, which was consistent with complete HM. The neonate showed a normal growth without any congenital anomalies. To date, 3 months after the delivery, the mother shows no clinical signs of persistent gestational trophoblastic disease.

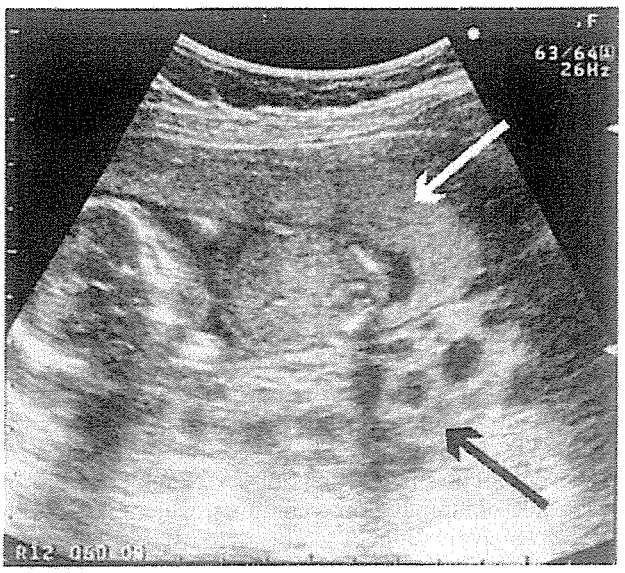

Fig. 1 Ultrasound image at 16 weeks of gestation. The presence of a normal placenta (*white arrow*) as well as of a fetus and separated cystic parts suggesting molar tissues (*black arrow*) are noted

Genetic analysis

Standard chromosomal analysis was performed using blood leukocytes of the mother, father, and newborn, and tissues from a normal placenta (three different sites), umbilical cord, and molar tissues. When the chromosomal analysis was not successful, fluorescence in situ hybridization (FISH) analysis using the probes specific for the X and Y chromosomes on uncultured cells was performed. All procedures were carried out after obtaining the written informed consent of the parents.

A QuickGene DNA whole blood kit (Fujifilm, Tokyo, Japan) was used to isolate genomic DNA from peripheral blood leukocytes of the mother and her husband and from umbilical cord blood leukocytes, and DNeasy Tissue kits (Qiagen, Valencia, Calif.) were used to isolate genomic DNA from tissues of the umbilical cord, normal placenta at three different portions, and molar tissues. Microsatellite analysis was carried out using ABI Prism linkage mapping set ver. 2.5, MD10 (Applied Biosystems, Foster City, Calif.) (Table 1). A total of 14 probes that mapped close to the centromere at *D6S422*, *D7S493*, *D8S285*, *D9S161*, *D10S208*, *D11S987*, *D12S345*, *D16S503*, *D17S1868*, *D17S921*, *D18S53*, *D19S220*, *D20S196*, and *DXS990* were used for this study. The PCR analysis was carried out on 10 μl aliquots of 10 ng genomic DNA, 0.5 μM of each primer, 0.2 mM each dNTP, 10× PCR buffer (Takara, Ohtsu, Japan), and 0.25 U of Takara Ex Taq DNA polymerase (Takara) under the following conditions: 40 cycles of 30 s at 94°C, 30 s at 55°C, 30 s, at 72°C. The PCR products were analyzed on an ABI 3100 Genetic Analyzer (Applied Biosystems), and their sizes were determined using the GENEMAPPER software ver 3.5 (Applied Biosystems).

Results and discussion

The karyotypes of the blood leukocytes from the father, mother, and newborn, and from the molar tissues and

Table 1 Microsatellite analysis

Markers[a]	Genotype											
	Father		Mother		Mole		Neonate		Cord		Placenta	
D6S422	1	2	3	2	1	1	3	2	3	2	3	2
D7S493	1	2	1	3	2	2	1	2	1	2	1	2
D8S285	1	2	3	3	1	1	3	1	3	1	3	1
D9S161	1	2	1	1	2	2	1	1	1	1	1	1
D10S208	1	2	2	2	2	2	2	2	2	2	2	2
D11S987	1	2	1	1	2	2	1	1	1	1	1	1
D12S345	1	2	1	2	1	1	1	2	1	2	1	2
D16S503	1	1	1	2	1	1	1	2	1	2	1	2
D17S1868	1	1	1	1	1	1	1	1	1	1	1	1
D17S921	1	2	3	2	1	1	1	2	1	2	1	2
D18S53	1	2	3	1	2	2	3	2	3	2	3	2
D19S220	1	2	2	2	2	2	1	2	1	2	1	2
D20S196	1	2	3	2	2	2	1	2	1	2	1	2
DXS990	1		2	3	1	1	1	3	1	3	1	3

[a]Different alleles in each marker are numbered arbitrarily. Paternal isodisomy was recognized at *D6S422*, *D7S493*, *D8S285*, *D9S161*, *D11S987*, *D17S921*, and *D18S53*

an umbilical cord tissue were 46,XY, 46,XX, 46,XX, 46,XX, and 46,XX, respectively. The chromosomal analysis of three sites of normal placental tissues was not successful due to bacterial contaminations. Subsequent FISH analysis of 50 uncultured cells of placental tissues using probes of the X and Y chromosomes only showed two signals of X chromosomes in all cells, indicating that the karyotype of the placenta was 46,XX (data not shown).

Molecular analysis showed that genomic DNA of the newborn, a cord tissue, and placental tissues showed a uniform pattern in which biparental genomes contributed in a Mendelian fashion. However, the molar tissue indicated paternal isodisomy at seven markers, *D6S422*, *D7S493*, *D8S285*, *D9S161*, *D11S987*, *D17S921*, and *D18S53*, suggesting that the molar tissues resulted from a doubling of a haploid paternal genome following monospermic fertilization of an inactivated oocyte. Indeed, most cases of complete HM have been described as being paternally uniparental 46,XX (homozygous constitution derived from the father), with only rare cases of the dispermic 46,XX or 46,XY conditions. In addition, the 46,YY constitution has never been described, probably because of early death of the conceptus (Reubinoff et al. 1997; Fisher et al. 2000). In this case, dispermic complete HM had been prevented by ICSI using a single spermatozoon. It should be noted that complete HM occurred irregardless of the presence of a morphologically normal embryo. There seems to be no way to differentiate HM from a normal embryo at the pre-transfer stage, although such a risk is very rare. Furthermore, the management of HM and a coexisting fetus is complicated. It is important to avoid a risk of a multiple pregnancy in ART by performing a single-embryo transfer.

In conclusion, we experienced a twin pregnancy with complete HM and a coexisting fetus following ICSI conception. To our best knowledge, this is the second report of this condition following ICSI (Petignat et al. 2001), but the first comprehensive genetic analysis.

Acknowledgements We kindly express our gratitude to Ms. Tamae Hanai for her excellent technical assistance.

References

Fisher RA, Khatoon R, Paradinas FJ, Roberts AP, Newlands ES (2000) Repetitive complete hydatidiform mole can be biparental in origin and either male or female. Hum Reprod 15:594–598

Jacobs PA, Szulman AE, Funkhouser J, Matsuura JS, Wilson CC (1982) Human triploidy: relationship between parental origin of the additional haploid complement and development of partial hydatidiform mole. Ann Hum Genet 46:223–231

Jones WB, Lauersen NH (1975) Hydatidiform mole with coexistent fetus. Am J Obstet Gynecol 122:267–272

Kajii T, Ohama K (1977) Androgenetic origin of hydatidiform mole. Nature 268:633–634

Matsui H, Sekiya S, Hando T, Wake N, Tomoda Y (2000) Hydatidiform mole coexistent with a twin live fetus: a national collaborative study in Japan. Hum Reprod 15:608–611

McDonald TW, Ruffolo EH (1983) Modern management of gestational trophoblastic disease. Obstet Gynecol Surv 38:67–83

Pal L, Toth TL, Leykin L, Isaacson KB (1996) High incidence of triploidy in in-vitro fertilized oocytes from a patient with a previous history of recurrent gestational trophoblastic disease. Hum Reprod 11:1529–1532

Petignat P, Senn A, Hohlfeld P, Blant SA, Laurini R, Germond M (2001) Molar pregnancy with a coexistent fetus after intracytoplasmic sperm injection. A case report. J Reprod Med 46:270–274

Reubinoff BE, Lewin A, Verner M, Safran A, Schenker JG, Abeliovich D (1997) Intracytoplasmic sperm injection combined with preimplantation genetic diagnosis for the prevention of recurrent gestational trophoblastic disease. Hum Reprod 12:805–808

Ruiz-Casares E, Henriques-Gil N, Opera M, Fernandez-Pacheco RP, Aguaron A (2001) Molecular analysis of a gestation consisting of a complete hydatidiform mole and normal dizygotic twin. J Reprod Med 46:1041–1045

nature genetics

Germline *KRAS* and *BRAF* mutations in cardio-facio-cutaneous syndrome

Tetsuya Niihori[1], Yoko Aoki[1], Yoko Narumi[1], Giovanni Neri[2], Hélène Cavé[3], Alain Verloes[3], Nobuhiko Okamoto[4], Raoul C M Hennekam[5], Gabriele Gillessen-Kaesbach[6], Dagmar Wieczorek[6], Maria Ines Kavamura[7], Kenji Kurosawa[8], Hirofumi Ohashi[9], Louise Wilson[10], Delphine Heron[11], Dominique Bonneau[12], Giuseppina Corona[13], Tadashi Kaname[14], Kenji Naritomi[14], Clarisse Baumann[3], Naomichi Matsumoto[15], Kumi Kato[1,16], Shigeo Kure[1] & Yoichi Matsubara[1,16]

Cardio-facio-cutaneous (CFC) syndrome is characterized by a distinctive facial appearance, heart defects and mental retardation. It phenotypically overlaps with Noonan and Costello syndrome, which are caused by mutations in *PTPN11* and *HRAS*, respectively. In 43 individuals with CFC, we identified two heterozygous *KRAS* mutations in three individuals and eight *BRAF* mutations in 16 individuals, suggesting that dysregulation of the RAS-RAF-ERK pathway is a common molecular basis for the three related disorders.

Cardio-facio-cutaneous (CFC) syndrome (OMIM 115150) was first described in 1986 (ref. 1). Affected individuals present with heart defects, including pulmonic stenosis, atrial septal defects and hypertrophic cardiomyopathy, and ectodermal abnormalities such as sparse, friable hair, hyperkeratotic skin lesions and a generalized ichthyosis-like condition. Typical facial characteristics include high forehead with bitemporal constriction, hypoplastic supraorbital ridges, downslanting palpebral fissures, a depressed nasal bridge and posteriorly angulated ears with prominent helices. The molecular basis of CFC syndrome has remained unknown. There are phenotypic similarities between this syndrome, Noonan syndrome (OMIM 163950) and Costello syndrome (OMIM 218040)[2,3]. Gain-of-function mutations in protein tyrosine phosphatase SHP-2 (*PTPN11*) have been identified in approximately 40% of individuals with clinically diagnosed Noonan syndrome[4]. No *PTPN11* mutations have been found in individuals with CFC syndrome[5–7]. Recently, we identified *HRAS* mutations in 12 of 13 individuals with Costello syndrome[8]. These findings suggest that the activation of the RAS-MAPK pathway is the common underlying mechanism of Noonan syndrome and Costello syndrome and, hence, possibly of CFC syndrome.

To elucidate the molecular basis of CFC syndrome, we first sequenced the entire coding regions of three RAS genes, *HRAS* (NC_000011), *KRAS* (NC_000012) and *NRAS* (NC_000001), in genomic DNA from 43 individuals with CFC syndrome (**Supplementary Methods** online). We identified two *KRAS* mutations: G60R (178G→C) in CFC73 and D153V (458A→T) in CFC8 and CFC91 (**Fig. 1a** and **Table 1**). Neither mutation has been previously identified in individuals with cancer (Sanger Institute Catalogue of Somatic Mutations in Cancer (COSMIC); http://www.sanger.ac.uk/cosmic). Gly60 and Asp154 are evolutionally conserved or chemically similar (**Supplementary Fig. 1** online). Neither of the two mutations was observed in 100 control chromosomes (data not shown). Their parents did not carry the mutations (**Supplementary Fig. 1**). The D153V mutation was identified in DNA extracted from both blood and buccal cells of individual CFC91. These results suggest that these germline mutations occurred *de novo*. No mutations in *KRAS*, *NRAS* or *HRAS* were found in the other 40 individuals with CFC syndrome.

Next, we examined the downstream molecules of RAS in the signaling pathway. The *RAF* proto-oncogene family consists of three isoforms, *CRAF*, *BRAF* and *ARAF*, and encodes for cytoplasmic serine/threonine kinases that are activated by binding RAS. Among these RAF molecules, BRAF is expressed at high levels in the brain and mutations in *BRAF* have been identified in 7% of all cancers[9]. We sequenced the entire 18 coding exons of *BRAF* (NC_000007) in 40 individuals with CFC syndrome and identified eight mutations in sixteen individuals (**Table 1**). Six mutations were located in the kinase domain (**Fig. 1b**). A G469E (1406G→A) mutation, which resides in the glycine-rich loop where somatic mutations are clustered in cancer, was identified in four individuals (CFC76, CFC81, CFC94 and CFC114). N581D (1741A→G), located in the catalytic loop, was identified in CFC95 and CFC110. Four mutations in the kinase domain between the glycine-rich loop and the catalytic loop were identified in five affected individuals: L485F (1455G→C) in CFC83, K499E (1495A→G) in CFC79, E501K (1501G→A) in CFC77 and E501G (1502A→G) in CFC90 and CFC105. A246P (736G→C) and

[1]Department of Medical Genetics, Tohoku University School of Medicine, Sendai, Japan. [2]Università Cattolica, Istituto di Genetica Medica, Rome, Italy. [3]Department of Genetics, Hôpital Robert Debré (APHP), Paris, France. [4]Department of Planning and Research, Osaka Medical Center and Research Institute for Maternal and Child Health, Izumi, Osaka, Japan. [5]Clinical and Molecular Genetics Unit, Institute of Child Health, London, UK and Department of Pediatrics, Academic Medical Center, Amsterdam, Netherlands. [6]Institut für Humangenetik, Universität Essen, Essen, Germany. [7]Medical Genetics Center, Federal University of Sao Paulo (UNIFESP), Sao Paulo, Brazil. [8]Division of Medical Genetics, Kanagawa Children's Medical Center, Yokohama, Japan. [9]Division of Medical Genetics, Saitama Children's Medical Center, Saitama, Japan. [10]Great Ormond Street Hospital, London, UK. [11]Genetic Department, Pitie-Salpetriere University Hospital, Paris, France. [12]Genetic Department, University Hospital, Angers, France. [13]Unità Operativa Complessa Patologia Neonatale e Terapia Intensiva, Dipartimento di Scienze Pediatriche Mediche e Chirurgiche, Azienda Ospedaliera Universitaria G. Martino, Messina, Italy. [14]Department of Medical Genetics, University of the Ryukyus School of Medicine, Okinawa, Japan. [15]Department of Human Genetics,Yokohama City University Graduate School of Medicine, Yokahama, Japan. [16]Comprehensive Research and Education Center for Planning of Drug Development and Clinical Evaluation, 21st Century COE Program, Tohoku University, Sendai, Japan. Correspondence should be addressed to Y.A. (aokiy@mail.tains.tohoku.ac.jp).

Received 20 November 2005; accepted 17 January 2006; published online 12 February 2006; doi:10.1038/ng1749

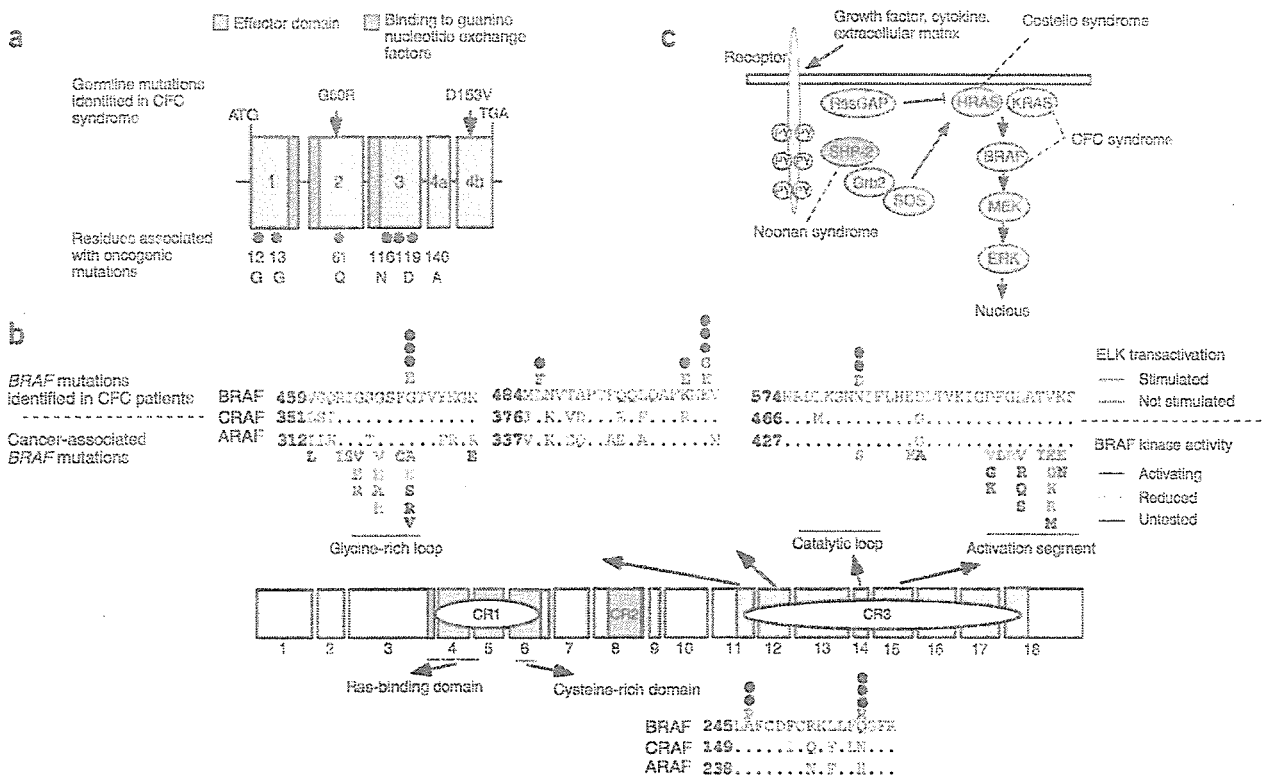

Figure 1 Mutations in *KRAS* and *BRAF* were identified in individuals with CFC syndrome. **(a)** Domain organization and genomic structure of the *KRAS* gene. Coding exons are numbered. In 98% of the transcripts, exon 4a is spliced out and only exon 4b is available for translation into protein. **(b)** *BRAF* consists of 18 exons. The three regions conserved in all RAF proteins (conserved region (CR) 1, CR2, and CR3) are shown in blue, green and yellow, respectively. The kinase domain is located in the CR3 domain. Six substitutions identified in CR3 are shown above. Filled circles indicate number of individuals having the substitution. Cancer-associated *BRAF* mutations are shown below the alignment of three RAF proteins[9,12]. Mutations detected in cancer are clustered in the glycine-rich loop and the activation segment of CR3 domain. The V600E mutation accounts for over 90% of the mutations in melanoma and thyroid cancer. Two mutations in the cysteine-rich domain were identified in five CFC individuals. Amino acids in CRAF and ARAF that are conserved in BRAF are shown by dots[13]. **(c)** RAS-ERK signaling pathway and associated disorders. RAS binds and stimulates RAF activation, which then activates MEK, which in turn activates ERK. ERK regulates gene expression and cytoskeletal rearrangements to coordinate the response to extracellular signals and regulate proliferation, differentiation, senescence and apoptosis[8,9]. Substitutions in *PTPN11*, *HRAS*, *KRAS* or *BRAF*, which potentially dysregulate the RAS-ERK signaling pathway, account for similar developmental disorders.

Q257R (770A→G), located in the cysteine-rich domain, were identified in five patients (**Fig. 1b** and **Table 1**). The identified eight substitutions were not found in 100 control chromosomes (data not shown). Mutation analysis in parents of five individuals (CFC76, CFC77, CFC96, CFC103 and CFC114) showed that these mutations occurred *de novo* (**Supplementary Fig. 2** online). The identified *BRAF* mutations were located in exons 6, 11, 12 and 14, and these domains were highly conserved in *CRAF* and *BRAF*. Sequencing of four corresponding exons in *CRAF*, ubiquitously expressed RAF, did not show any mutations in 24 individuals (data not shown).

KRAS and BRAF molecules are the key regulators of the RAS-RAF-MEK-ERK pathway, which is important for proliferation, growth and death of cells[9]. To elucidate critical steps, we examined the effect of the identified mutations on the RAS-ERK pathway by studying the activation of the ELK transcription factor. We transfected expression constructs (*KRAS* cDNA, NM_004985; *BRAF* cDNA, NM_00433) with a pFR-luc *trans*-reporter vector, a pFA2-ELK1 vector and a phRLnull-luc vector in NIH3T3 cells and determined their relative luciferase activity (RLA). We observed a significant increase in RLA in cells transfected with *KRAS* D153V but not in cells transfected with *KRAS* G60R (**Supplementary Fig. 3** online). We observed a two- to fourfold increase in RLA in cells transfected with two *BRAF* mutations (A246P and Q257R) in the cysteine-rich domain as well as in cells transfected with two *BRAF* mutations (L485S and K499E) in the kinase domain. We did not observe any significant increase in RLA in the other four mutations. Protein blotting showed that the wild-type and mutant proteins of *KRAS* and *BRAF* were equally expressed (data not shown). These results suggest that one *KRAS* and four *BRAF* mutants identified in CFC syndrome stimulated a common signaling pathway.

We identified substitutions of two proto-oncogenes, *KRAS* and *BRAF*, in 44% of individuals with CFC syndrome, suggesting that *KRAS* and *BRAF* have similar roles in human development. Controversy has existed as to whether CFC and Noonan syndromes are distinct disorders or different phenotypes of the same condition[2,10]. The clinical data of the 19 mutation-positive CFC individuals showed a high frequency of growth failure (78.9%), mental retardation (100%), relative macrocephaly (78.9%), characteristic facial appearance, including bitemporal constriction (84.2%) and downslanting palpebral fissures (94.7%), curly sparse hair (100%), heart defects (84.2%) and skin abnormalities (68.4%) (**Supplementary Table 1** online). This is in contrast with Noonan syndrome, in which there are lower frequencies of mental retardation (24–35%), heart defects (50–67%) and skin

Table 1 Mutations in 19 individuals with CFC syndrome

Individual	Gene	Exon	Nucleotide substitution	Amino acid change
CFC73	KRAS	2	178G→C	G60R
CFC8	KRAS	4b	458A→T	D153V
CFC91	KRAS	4b	458A→T	D153V
CFC100	BRAF	6	736G→C	A246P
CFC103	BRAF	6	736G→C	A246P
CFC16	BRAF	6	770A→G	Q257R
CFC24	BRAF	6	770A→G	Q257R
CFC96	BRAF	6	770A→G	Q257R
CFC76	BRAF	11	1406G→A	G469E
CFC81	BRAF	11	1406G→A	G469E
CFC94	BRAF	11	1406G→A	G469E
CFC114	BRAF	11	1406G→A	G469E
CFC83	BRAF	12	1455G→C	L485F
CFC79	BRAF	12	1495A→G	K499E
CFC77	BRAF	12	1501G→A	E501K
CFC90	BRAF	12	1502A→G	E501G
CFC105	BRAF	12	1502A→G	E501G
CFC95	BRAF	14	1741A→G	N581D
CFC110	BRAF	14	1741A→G	N581D

abnormalities (2–27%)[2]. Mutation analysis of *PTPN11* was negative in 43 CFC individuals. We did not identify any mutations in any exons of *KRAS* or in exons 6, 11, 12 and 14 of *BRAF* in 26 individuals with *PTPN11*-negative Noonan syndrome (data not shown), suggesting that Noonan syndrome and CFC syndrome are distinct clinical entities.

Comparison of manifestations between *KRAS*-positive and *BRAF*-positive individuals showed similar frequencies of growth and mental retardation, craniofacial appearance, abnormal hair and heart defects (**Supplementary Tables 2** and **3** online). However, we did observe a difference between the two groups in manifestations of skin abnormality, including ichthyosis, hyperkeratosis and hemangioma, which were observed in 13 *BRAF*-positive individuals. In contrast, no *KRAS*-positive individuals had these skin problems ($P < 0.05$). Somatic mutations in *BRAF* were identified in 60% of malignant melanoma or nevi[9], suggesting that BRAF has an important role in the skin. Comparison of manifestations between individuals with mutations that induced ELK transactivation and those with mutations that did not induce ELK transactivation showed no significant differences. Further analysis in a larger cohort would clarify the genotype-phenotype relationship in affected individuals.

The crystal structure of the BRAF kinase domain showed that the six *BRAF* mutations identified in this study are located in the interface of the ATP binding cleft, suggesting that these mutations may alter the catalytic activity of kinase domain (**Supplementary Fig. 4** online). Luciferase assays showed that two mutations (L485F and K499E) stimulated ELK-dependent transcription, suggesting that these mutants activated the ERK pathway. Missense mutations of *BRAF* were identified in approximately 7% of cancers, including human malignant melanoma and colorectal cancer[9]. The most frequent (>90%) V600E mutant showed elevated kinase activity, resulting in the activation of ERK and increased transformation activity[11]. Other less frequent mutations identified in cancer had either elevated or reduced kinase activity[9]. The four mutations identified in the kinase domain in our study did not enhance ELK-dependent transcription. This is in agreement with recent studies reporting that the activation of ERK or ELK transcription was not observed in cancer-associated mutations, including G469E (ref. 12). In cancer, *BRAF* mutations other than V600E are sometimes coincident with *RAS* mutations[9]. Other genetic background may contribute to the pathogenesis of CFC syndrome, although we did not detect any mutations in *KRAS*, *HRAS* or *NRAS* in *BRAF*-positive individuals. Further functional analysis of *BRAF* mutations will help elucidate the effects of these mutations on cell signaling.

The A246P and Q257R mutations are the first to be identified in the cysteine-rich domain in *BRAF*. This cysteine-rich domain is adjacent to the RAS-binding domain in conserved region 1 (ref. 13). A past study has suggested that the cysteine-rich domain of CRAF not only binds activated small GTPase RAS, but also inhibits basal catalytic RAF activity by direct or indirect interaction with the catalytic domain[14]. Our luciferase assay showed that these two mutations significantly activated ELK-dependent transcription, suggesting that they contribute to the activation of *BRAF*, leading to stimulation of the RAS-ERK pathway.

Previous clinical reports have shown that the association with cancers is rare in CFC syndrome[15]. This is in contrast with individuals with Costello syndrome, who have a higher risk of cancer, including rhabdomyosarcoma, ganglioneuroblastoma and bladder carcinoma[8]. It is of note that individual CFC94 with a *BRAF* G469E mutation had acute lymphoblastoid leukemia[15]. Careful observation of affected individuals would clarify the possible predisposition to hematopoietic malignancy in CFC syndrome as described in Noonan syndrome[4].

To the best of our knowledge, this is the first report of germline mutations in *KRAS* and *BRAF*. Our results suggest that mutations in human oncogenes (*HRAS*, *KRAS*, *BRAF* and *PTPN11*) that potentially dysregulate the RAS-MAPK pathway represent a common fundamental mechanism of related developmental disorders, namely, Noonan syndrome, Costello syndrome and CFC syndrome (**Fig. 1c**).

GenBank accession numbers. *KRAS* coding region, NC_000012; *HRAS* coding region, NC_000011; *NRAS* coding region, NC_000001; *BRAF*, NC_000007; *KRAS* cDNA, NM_004985; *BRAF* cDNA, NM_004333.

Note: Supplementary information is available on the Nature Genetics website.

ACKNOWLEDGMENTS

We wish to thank the individuals and their families who participated in this study and the doctors who referred the cases. The support of CFC International in facilitating the collection of patient samples is gratefully acknowledged. We are grateful to J. Miyazaki, Osaka University, for supplying the pCAGGS expression vector. This work was supported by Grants-in-Aid from the Ministry of Education, Culture, Sports, Science and Technology of Japan and Grants-in-Aid from the Ministry of Health, Labor, and Welfare of Japan.

COMPETING INTERESTS STATEMENT

The authors declare that they have no competing financial interests.

Published online at http://www.nature.com/naturegenetics
Reprints and permissions information is available online at http://npg.nature.com/reprintsandpermissions/

1. Reynolds, J.F. *et al. Am. J. Med. Genet.* **25**, 413–427 (1986).
2. Wieczorek, D., Majewski, F. & Gillessen-Kaesbach, G. *G. Clin. Genet.* **52**, 37–46 (1997).
3. van Eeghen, A.M., van Gelderen, I. & Hennekam, R.C. *Am. J. Med. Genet.* **82**, 187–193 (1999).
4. Tartaglia, M. & Gelb, B.D. *Eur. J. Med. Genet.* **48**, 81–96 (2005).
5. Ion, A. *et al. Hum. Genet.* **111**, 421–427 (2002).
6. Kavamura, M.I. *et al. Eur. J. Hum. Genet.* **11**, 64–68 (2003).
7. Musante, L. *et al. Eur. J. Hum. Genet.* **11**, 201–206 (2003).
8. Aoki, Y. *et al. Nat. Genet.* **37**, 1038–1040 (2005).
9. Garnett, M.J. & Marais, R. *Cancer Cell* **6**, 313–319 (2004).
10. Neri, G., Zollino, M. & Reynolds, J.F. *Am. J. Med. Genet.* **39**, 367–370 (1991).
11. Davies, H. *et al. Nature* **417**, 949–954 (2002).
12. Ikenoue, T. *et al. Cancer Res.* **64**, 3428–3435 (2004).
13. Mercer, K.E. & Pritchard, C.A. *Biochim. Biophys. Acta* **1653**, 25–40 (2003).
14. Winkler, D.G. *et al. J. Biol. Chem.* **273**, 21578–21584 (1998).
15. van Den Berg, H. & Hennekam, R.C. *J. Med. Genet.* **36**, 799–800 (1999).

J Hum Genet (2006) 51:533–540
DOI 10.1007/s10038-006-0394-5

ORIGINAL ARTICLE

**Hisashi Sato · Toshinobu Miyamoto · Leah Yogev
Mikio Namiki · Eitesu Koh · Hiroaki Hayashi
Yoshihito Sasaki · Mutsuo Ishikawa · Dolores J. Lamb
Naomichi Matsumoto · Ohad S. Birk · Norio Niikawa
Kazuo Sengoku**

Polymorphic alleles of the human *MEI1* gene are associated with human azoospermia by meiotic arrest

Received: 18 October 2005 / Accepted: 14 February 2006 / Published online: 9 May 2006

Abstract Genetic mechanisms are implicated as a cause of some male infertility, yet are poorly understood. Mouse meiotic mutant mei1 (meiosis defective 1) was isolated by a screening of infertile mice. Male mei1 mice have azoospermia due to meiotic arrest, and the mouse *Mei1* gene is responsible for the mei1 phenotype. To investigate whether human *MEI1* gene defects are associated with azoospermia by meiotic arrest, we isolated the human *MEI1* cDNA based on the mouse Mei1 amino acid sequence. *MEI1* is expressed specifically in the testis. Mutational analysis by direct sequencing of all *MEI1* coding regions was performed in 27 men (13 European Americans, 13 Israeli and 1 Japanese) having azoospermia due to complete early meiotic arrest. This identified four novel, coding single-nucleotide-polymorphisms (cSNPs), i.e., SNP1 (T909G), SNP2 (A1582G), SNP3 (C1791A) and SNP4 (C2397T) in exons 4, 8, 9 and 14, respectively. Using these cSNPs, an association study was carried out between 26 non-Japanese patients with azoospermia and two sets of normal control men (61 normal European Americans and 60 Israelis). Consequently, SNP3 and SNP4 were shown to be associated with azoospermia among European Americans ($P = 0.0289$ and $P = 0.0299$ for genotype and allele frequencies at both the polymorphic sites, respectively), although no such association was observed among Israelis ($P > 0.05$). Haplotype estimation revealed that the frequencies of SNP3–SNP4 (C–T), SNP3–SNP4 (A–C) and SNP3–SNP4 (A–T) were higher in the European American patients, and the frequency of SNP3–SNP4 (A–T) was also higher than in both control groups. These results suggest that *MEI1* may play a role in meiosis during spermatogenesis, especially in European Americans.

Keywords Azoospermia · Infertility · MEI1 · Meiosis · Polymorphisms

H. Sato · T. Miyamoto (✉) · H. Hayashi · Y. Sasaki
M. Ishikawa · K. Sengoku
Department of Obstetrics and Gynecology,
Asahikawa Medical College, 2-1-1-1 Midorigaokahigashi,
Asahikawa 078-8510, Japan
E-mail: toshim@asahikawa-med.ac.jp
Tel.: +81-166-682562
Fax: +81-166-682569

L. Yogev
Institute for the Study of Fertility, Lis Maternity Hospital,
Tel Aviv Sourasky Medical Center, Tel Aviv, Israel

M. Namiki · E. Koh
Department of Urology, Kanazawa University Graduate School of Medical Science, Kanazawa, Japan

D.J. Lamb
Scott Department of Urology, and Department of Molecular and Cellular Biology, Baylor College of Medicine, Houston, TX, USA

O.S. Birk
Department of Molecular Developmental Genetics,
Faculty of Health Sciences, Ben-Gurion University of the Negev,
Beer-Sheva, Israel

N. Matsumoto
Department of Human Genetics,
Yokohama City University Graduate School of Medicine,
Yokohama, Japan

N. Niikawa
Department of Human Genetics,
Nagasaki University Graduate School of Biomedical Sciences,
Nagasaki, Japan

N. Niikawa
SORST, JST, Kawaguchi, Japan

Introduction

Genetic causes of severe male infertility include chromosomal abnormalities such as Y-chromosome microdeletions and specific gene mutations in *AZF, DAZ, RBMY, USP9Y* and *SYCP3* (Reijo et al. 1995; Elliott et al. 1997; Sun et al. 1999; Matzuk and Lamb 2002;

Miyamoto et al. 2003). Since the Y-chromosome deletions explain only up to 21% of men with infertility (Nakamura et al. 2001), azoospermia in many infertile men may be caused by autosomal gene mutations. Genetic polymorphisms may also be factors susceptible to some forms of male infertility, albeit somewhat controversially, e.g., whether the CAG repeat of the human androgen-receptor gene is linked to male infertility (Dowsing et al. 1999).

Defective meiosis during spermatogenesis is one of the critical causes of azoospermia, although the details remain unknown. In sexually reproducing species, meiosis is a fundamental process that allows a genetic exchange between maternal and paternal genomes (Nasmyth 2002). The genetic regulation of meiosis in mammals is poorly understood compared to that in lower eukaryotes such as yeast. Several key genes expressed in mouse meiosis, including *Dmc1*, *Fkbp6*, *Scp3* (*Sycp3*), *Spo11*, *Msh4* and *Msh5*, have been identified by disruption experiments in embryonic stem (ES) cells (Yoshida et al. 1998; Pittman et al. 1998; Edelmann et al. 1999; Baudat et al. 2000; Kneitz et al. 2000; Romanienko and Camerini-Otero 2000; Yuan et al. 2000; Crackower et al. 2003). In addition, the mouse meiotic mutant mei1 (meiosis defective 1) was isolated by a screening of infertile mice generated by chemical mutagenesis in ES cells (Munroe et al. 2000). The male mice mutant for the *Mei1* gene has small testes and lacks the epididymal sperm and postmeiotic cells. The seminiferous tubules of such mice contain spermatocytes arrested at the zygotene/pachytene stage of meiosis (Libby et al. 2003). In contrast, few genes essential to human meiosis are known.

In the present study, we isolated the human *MEI1* cDNA using the deduced amino acid sequence of the mouse *Mei1* cDNA, and analyzed a possible association of *MEI1* mutations with azoospermia by meiotic arrest in man.

Materials and methods

Isolation of the human *MEI1* cDNA and analysis of its expression in various tissues

The mouse *Mei1* cDNA was isolated previously (Libby et al. 2003). Using the mouse Mei1 amino acid sequence (GenBank accession no. AY270177), we identified its homologous region in the human genome (GenBank BX391221). We designed a pair of primers (MEI1F2 and MEI1R2) in the human homologous region encompassing the putative introns, and carried out PCR on a human testis cDNA library (Clontech, Tokyo, Japan). The sequences (5′–3′) of the oligonucleotides used were as follows: MEI1F2, GCTGGAAGAAGCCATGCAGG; and MEI1R2, AGTCCGGTCCCTGGTCATTG. Semi-nested PCR was performed with MEI1F2/MEI1R3 and a 10-fold dilution of the first PCR product as a template. The other oligonucleotide (5′–3′) used was MEI1R3, TGCAGAACCTCCTGGTGCAG. The product from the semi-nested PCR was subcloned into a T-Easy vector (Promega, Madison, WI), and several representative clones were sequenced in both directions. The 5′- and 3′-RACE were performed with primers 5RAFUL1, 5RAFUL8, 3RA1, 3RA5, AP1 (Clontech) and AP2 (Clontech). Their sequences (5′–3′) were as follows: 5RAFUL1, GTACTGGCGATCAGACAGGAAGGCAAGG; 5RAFUL8, AAGGATGAGGAAGCTTCAGAGCCGTGGG; 3RA1, TGGATGCTGGAGAGAATTCCTTCCTCAG and 3RA5, TTTGGCTGACCTGTCTACCCTCTCGAAC. Both RACE products were also subcloned, and several representative clones were sequenced in both directions. The isolated full-length cDNA sequences were compared with human genomic sequences. All PCRs were carried out using an Advantage 2 PCR Kit (Clontech) under the following conditions and according to the manufacturer's instructions: initial denaturation at 95°C for 150 s, followed by 32 cycles of denaturation at 95°C for 15 s, annealing and extension at 68°C for 90 s.

For expression analysis of *MEI1*, PCR of cDNA from various tissue types (spleen, thymus, prostate, testis, ovary, small intestine, colon, leukocyte, brain, heart, kidney, liver, lung, pancreas and placenta) purchased from Clontech was performed with EXP2F1 and EXP2R6 as primers. The sequences (5′–3′) of the primers were: EXP2F1, CTGGGAAGAGAGCAGCTATG; and EXP2R6, CTGCTGGGTGTGGTCTGATG. PCR conditions were initial denaturation at 95°C for 150 s, followed by 32 cycles of denaturation at 95°C for 15 s, annealing and extension at 68°C for 90 s using an Advantage 2 PCR Kit.

Patients and control individuals

All patients and donors participating in this study gave informed consent for molecular analysis of their blood samples, and the study protocol was approved by the Committee for the Ethical Issues on Human Genome and Gene Analysis, Tel Aviv Sourasky Medical Center and Kanazawa University. To test the hypothesis that human *MEI1* gene mutations are associated with human azoospermia, we screened 27 patients diagnosed as having azoospermia due to complete meiotic arrest. Genomic DNA from 13 of these patients was obtained from the NIH funded tissue bank at Baylor College of Medicine with the patients' written informed consent and the full oversight of the Institutional Review Boards for the Protection of Human Subjects at Baylor College of Medicine. These men underwent clinical evaluations for diagnosis and treatment of their azoospermia by an expert diagnostician, Dr. Larry Lipshultz. They provided an extensive history and underwent a physical examination, as well as state-of-the-art andrology testing (showing a normal karyotype by high resolution banding chromosome analysis and by testing for Y-chromosome microdeletions). Consequently, azoospermia was

diagnosed to be idiopathic in all cases. Of the 27 patients, 13 were European Americans, 13 were from Israel and the remaining 1 was from Japan, and all had normal karyotypes and no Y-chromosome microdeletions. Pathological examination of bilateral testicular biopsy specimens from 26 (13 European Americans and 13 Israelis) of the 27 men showed an early maturation arrest testicular phenotype (the most mature spermatogenic cell type present was the spermatocyte), which was consistent with that seen in mei1 mutant mice. Sixty-one and 60 healthy and pregnancy-proven fertile men (European American and Israeli, respectively) were used as normal control individuals.

MEI1 mutation screening

To test the hypothesis that *MEI1* gene mutations are associated with human non-obstructive azoospermia, we screened 27 patients for mutations in *MEI1*. Genomic DNA was obtained from peripheral blood lymphocytes using a Qiagen Blood and Cell Culture DNA Midi Kit (Qiagen, Hilden, Germany). After all exon–intron borders were identified by comparison between the full-length cDNA and genomic sequences (NT_007758.10), all *MEI1* coding regions and intronic sequences adjacent to exons of the patients were analyzed by direct sequencing. Nested or semi-nested PCRs were performed using primers for each intronic region (Table 1) and 10-fold diluted first PCR products as templates. PCR was performed in a final volume of 25 μl, consisting of genomic DNA (10 ng), dNTP (0.32 mM each) (TaKaRa, Shiga, Japan), each primer (0.2 mM), *Taq* polymerase (0.625 U) (Roche, Tokyo, Japan) and reaction buffer containing $MgCl_2$ (Roche). Nested and semi-nested PCRs were carried out for 20 cycles under the same conditions above but with 2 μl of 10-fold diluted first PCR products as templates, using a programmable PC 960G gradient thermal cycler (Cosmo Bio, Tokyo, Japan) using the following PCR conditions: initial denaturation at 95°C for 150 s, followed by 32 cycles of denaturation at 95°C for 30 s, annealing at (primer T_m−5°C) for 90 s and extension at 72°C for 90 s. PCR products were purified using a QIAquick PCR Purification kit (Qiagen), and direct sequencing of each product was carried out in both directions.

Genotyping and statistical analyses

Single-locus analysis

To investigate the role of *MEI1* polymorphisms in azoospermia, 26 patients (13 European Americans and 13 Israelis) were genotyped for polymorphic alleles, and compared to the genotype and allele frequencies in the normal control men. To match ethnic populations, the single Japanese patient was excluded from the study.

Table 1 Sequences of oligonucleotide primers used for mutation analysis

		Forward primer		Reverse primer
Exon2	E2F1	5′-CATAGCCACCTTAAGACCTC-3′	E2R1	5′-ATTCCTCTGGGCAGCCTCAG-3′
	E2F2	5′-ACTAGCCTCTGGCACAAAGC-3′	E2R2	5′-TCGTGGCTGTACTAACTCAC-3′
Exon3	E3F1	5′-TCCCGGTAGGTTGAACCTTG-3′	E3R1	5′-CAGTGTCTACCCACCTGTTC-3′
	E3F2	5′-AAGAGGAGCCTCTGATTTCC-3′	E3R2	5′-AAGATATGAGCCTCTCAGGG-3′
Exon4	E4F1	5′-GAGTATTTGGCCCCTAACTG-3′	E4R1	5′-CTCCACACTCCTAACACCTC-3′
	E4F2	5′-GCACAAGGCACAGAACAATG-3′	E4R2	5′-CTCTCTCTACCACCCGCTTG-3′
Exon5	E5F1	5′-TCTCACTAAAGTGCCTTGGG-3′	E5R1	5′-GAGGTGGGCTGAAGCAGATG-3′
	E5F2	5′-GCCAAGGTGTCCTGGAATAC-3′	E5R2	5′-CTCAGTAAACCGGCTCTCAG-3′
Exon6	E6F1	5′-GGATGGACCTATTCTAAGGG-3′	E6R1	5′-GCAGTGAGAGAAAGGAGGTG-3′
	E6F2	5′-GCACCTAGAAGAGCCTTTGG-3′	E6R2	5′-CTTGATGCCACAATGGCCTG-3′
Exon7	E67F1	5′-GAAGTCACTCAGCCTCTCTG-3′	E67R1	5′-AGAGAAAGCCCTGAGAGGTC-3′
	E67F2	5′-TACCAACCTATGTCTGGCAC-3′	E67R2	5′-GGACAGACTGACCTACTAGC-3′
Exon8	E7F1	5′-CTAGATGGAGGGTGTGAATG-3′	E7R1	5′-GAGCCAGAAAGGACCTTATG-3′
	E7F2	5′-TTAGTTTGTGCTTGCTCCCC-3′	E7R2	5′-ACCAGCCACACACACAACCC-3′
Exon9	E8F1	5′-GAGCTTCTGTTATGAAGCTG-3′	E8R1	5′-CTAATAAGCCCCCAGAGCTG-3′
	E8F3	5′-TCAGGTGCTAAGCACCATAG-3′	E8R3	5′-TGCCACCCCATGCCTCAAAG-3′
Exon10	E9F1	5′-TGATTCTCCGCATGCTCCTG-3′	E9R1	5′-ATTATGGAGTGACCATTGGC-3′
	E9F2	5′-TTGGAGGACTCTGTGTGGCC-3′	E9R2	5′-GCTGGTCTTATCTGAAAACC-3′
Exon11	E10F1	5′-CCACAAGTCTCCAGCAGAAG-3′	E10R1	5′-GTCTTAATCCACCCTGGAAG-3′
	E10F2	5′-CAGATAAGACCAGCACCCTG-3′	E10R2	5′-GAGTATCAGGCTCTCGACAG-3′
Exon12	E11F1	5′-TACAGGCGTGAGCCACTCTG-3′	E11R1	5′-AGGGAATGGAAGGCTGGAGC-3′
	E11F3	5′-TGAGGGTGAGAGATGAAGCC-3′	E11R3	5′-CTCTCTCATGGGAACATCAG-3′
Exon13	E12F2	5′-CCTTGGGTCAGCTTGTTCAG-3′	E12R2	5′-TCTTCAGCACCACCCAGCTC-3′
	E12F3	5′-CCTGTCTCTAACTGGGTAGC-3′	E12R3	5′-GACACTCCTCAGACCACAAG-3′
Exon14	E13F1	5′-ACTCTGAGCTCCTTGAAGGC-3′	E13R1	5′-TTGCTGTGGCCAGAGCTCCC-3′
	E13F2	5′-CAGGTTCTGTGGGCTTCAGG-4′	E13R2	5′-AGAGAAGATGGTGTTGAGGG-3′
Exon15	E14F1	5′-TGCAGCCACTGTAAAGCTAG-3′	E14R1	5′-GAGAGAGGACACTGCTACTC-3′
	E14F2	5′-TTCTCTTGGAGGGTGGGAGC-3′	E14R2	5′-AACTGGCCCAGGAAGAGAAG-3′
Exon16	E15F1	5′-CATCCCACTATTCTCAGGAG-3′	E15R1	5′-CTCCTTGCTGAAACAATCCC-3′
	E15F2	5′-ACTTCTGTTCTTGCCTGACC-3′	E15R2	5′-ATCCAACTGGCTGAGAAACC-3′

Fisher's exact test was used to determine the significance of differences. P values of 0.05 or less were considered statistically significant. The Hardy–Weinberg equilibrium (HWE) was tested using a commercial program (SNPAlyze ver 5.0 Standard; Dynacom, Chiba, Japan).

Pairwise locus disequilibrium analysis

The measure of linkage disequilibrium (LD) known as D' (Lewontin 1988), which is corrected for allele frequencies of loci, was computed for allele at pairs of SNP loci using the 26 patients. Tests of departures from linkage equilibrium were performed using the composite test for the overall SNPs. P values were determined via χ^2 approximation. As described above, significance was determined at the $P = 0.05$ level. These calculations were performed using a commercial program (SNPAlyze ver 5.0 Standard).

Haplotype frequency estimation

Haplotype frequencies were estimated by the method of maximum likelihood from genotype data through the use of the expectation–maximization (E–M) algorithm under the assumption of HWE (Excoffier and Slatkin 1995). Haplotype-based hypothesis tests focused on the case and control groups. Haplotypes of SNP were assessed using the EH package soft (http://linkage.rockefeller.edu/soft/). Chi-square statistics were derived from a series of simple 2×2 tables based on the frequency of each haplotype versus all others combined between the case and control groups. P values were determined via χ^2 approximation. Significance was determined at the $P = 0.05$ level.

Results

Based on the amino acid sequence deduced from the mouse *Meil* cDNA, we have identified the human *MEI1* cDNA. Comparison of the cDNA and its corresponding genomic sequence revealed that *MEI1* is located to chromosome 22q13.2, consists of 16 exons encompassing over 47.1 kb in the genome, with an open reading frame (ORF) from nt 634 to 2,562 (Fig. 1). *MEI1* has at least two alternative transcripts of 2,714 and 2,609 bp (annotated as AY952376 and AY952377 in GenBank, respectively), encoding proteins of 642 and 607 amino acids, respectively. The shorter 2,609-bp cDNA lacks exon 7 as a result of alternative splicing. Furthermore, the 642 amino acid protein shares 77% homology with the mouse Mei1 protein (Fig. 2) and the cDNA in the coding region shares 61% homology with the mouse *Meil* cDNA. However, no previously known functional domains could be found in human MEI1. Analysis of expression patterns of *MEI1* in various adult tissues revealed that it was predominately expressed in the testis and weakly in the spleen and thymus (Fig. 3).

Mutation analysis of *MEI1* revealed four nucleotide changes among the 27 patients, i.e., T909G in exon 4, A1582G in exon 8, C1791A in exon 9 and C2397T in exon 14. As the four coding single nucleotide polymorphisms (cSNPs) were hitherto undescribed or have not been registered in the NCBI database, they are novel cSNPs (Table 2). Among SNP1 (T909G), SNP2 (A1582G), SNP3 (C1791A) and SNP4 (C2397T), the latter three SNPs were observed in the heterozygous state in all but the Japanese patient and SNP2 is nonsynonymous (Thr–Ala). We did not find any of these SNPs in the Japanese patient.

Genotyping for *MEI1* SNP alleles among the 26 patients (13 European Americans and 13 Israelis) and 61 control individuals (European Americans) revealed that the genotype distribution and the allele frequency of SNP3 and SNP4 were significantly different between the two groups (Table 2). At the 1791A/C site (SNP3), the proportions of AA homozygote/AC heterozygote/CC homozygote in the patient and control groups were 0.00/0.154/0.846 and 0.000/0.000/1.000, respectively ($P = 0.0067$). The allele frequencies for 1791A/C in the two groups were 0.077/0.923 and 0.00/1.000, respectively, and were significantly different ($P = 0.0073$). Likewise, at the 2397T/C site (SNP4), the proportions of

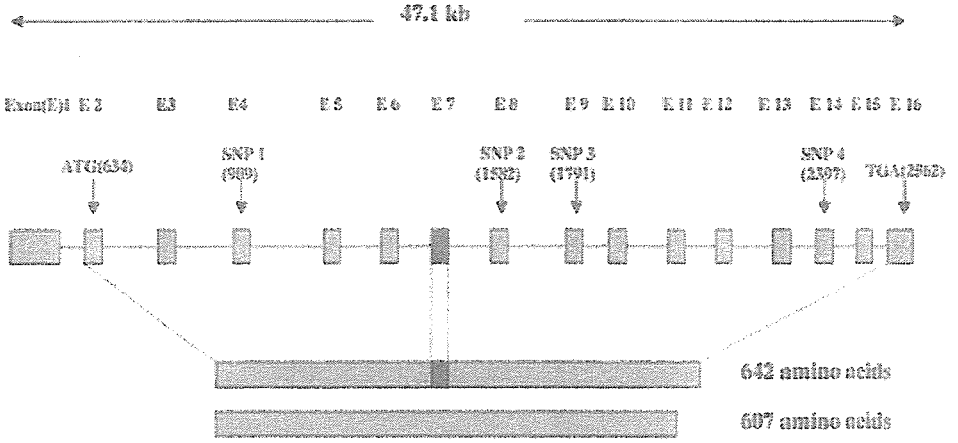

Fig. 1 Gene structure and four novel coding single-nucleotide-polymorphism (cSNP) sites in the human *MEI1* gene. The gene consists of 16 exons, and alternative splicing events generate two mRNA products. The shorter cDNA lacks exon 7. *Arrows* indicate four novel SNPs (SNP1, SNP2, SNP3 and SNP4), the start codon and the stop codon

```
human: 1   MCLNLLSAPEKTGPPSKEELSAVSELLQHGLPQISSRSPESLAFLSDRQYMEGAARQRQY 60
           ||||||||||||  | |  ||||||||  ||||||  ||||  ||||||||||||  | |  |||||
mouse: 254 MCLNLLSAPEKTEPLSQEELSAVSEFLQHGLPHISSRTPESLAFLSDRQYVEAATRQRQY 313

human: 61  CILLLFYLAYIHEDRFVSEAELFEAVQSFLLSLQDQGERPPLVVFKASIYLLAICQDKDN 120
           |||||||||  ||  ||||  |||||  ||||||||||||||  ||  ||  ||||||||  |  |||
mouse: 314 CILLLFYLAHIHDDRFVPEAELFVAVQSFLLSLQDQGECPPPVVCKASMYLLAVCGDKDS 373

human: 121 TLRETMVSAIRKFLEGIPDLQLVYTHHPLLLRFFLLYPELMSRYGHRVLELWFFWEESSY 180
             | |   ||||||||||||||  ||||||||||||| ||  ||||||||||||||  ||||  |
mouse: 374 ALAEAVISAIRKFLEGIPDLRGVYTHHPLLLRFFLAYPGLMSRFGHRVLELWFSWEESGY 433

human: 181 EELDDVTSAGQPALPASLVVLFQLLRSIPSILLILLDLIYSSPVDTAHKVLISLRTFLRR 240
           |  |||   | |     ||  |   ||   |  | ||||||||||  ||||||||  ||||  ||  ||
mouse: 434 ENLDDDSSPGRTVFPANLAALFRVLQSTPSILLILLDLVYSSPVDTARKVLIVLRVFLWE 493

human: 241 NEDIQVGGLIRGHFLLILQRLLVEHGASPSGASGNLPLLLSLLSLMQLRNVSEQELDSVA 300
           |||  ||||||||||||||||||||  ||   |   |||||||  ||||  |  ||  |||||||  |
mouse: 494 NEDVKVGGLIRGHFLLILQRLLVEYGA--STSGGNLPLLLNLLSLVQMRNESEQELDSMA 551

human: 301 MKLLHQVSKLCGKCSPTDVDILQPSFNFLYWSLHQTTPSSQKRAAAVLLSSTGLMELLEK 360
           ||||||||  |||||||  ||||||||||||||||||||||||||||||||||||||||  |  |||||
mouse: 552 MKLLHQVSMLCGKCSPAHVDILQPSFNFLYWSLHQTTPSSQKRAAAVLLSSTALLELLEK 611

human: 361 MLALTLAK-ADSPRTALLCSAWLLTASFSAQQHKGSLQVHQTLSVEMDQVLKALSFPKKK 419
           |||||       ||||  ||  ||||||||||||||  |  ||||  |||||   ||||||||||
mouse: 612 MLALTWTETGSSPRTPLLSSAWLLTASFSAQQHNGNLQVHRTLSVELNQVLKALSFPKKM 671

human: 420 AALLSAAILCFLRTALRQSFSSALVALVPSGAQPLPATKDTVLAPLRMSQVRSLVIGLQN 479
           ||||||||  ||||||  ||||||||  |||||  |||     |  |||||  |||  |  |||||
mouse: 672 SALLSAAILRFLRTALQQSFSSALVVLVPSGDQPLSTPEDAVLAPLGKSQVLALLIGLQN 731

human: 480 LLVQKDPLLSQACVGCLEALLDYLDARSPDIALHVASQPWNRFLLFTLLDAGENSFLRPE 539
           |||||||||||||||||||||||||  ||||||||||||||||||||||||||||||||||||
mouse: 732 LLVQKDPLLSQACIGCLEALLDYLHARSPDIALHVASQPWNRFLLFTLLDAGENSFLRPE 791

human: 540 ILRLMTLFMRYRSSSVLSHEEVGDVLQGVALADLSTLSNTTLQALHGFFQQLQSMGHLAD 599
           ||||||||  ||||  |||  ||||  |||  ||  |||  |||  ||||||||  |  ||||  |  |
mouse: 792 ILRLMTLFVQYRSSCVLSREEVGLILQGAALVDLSALSNDTLQALHGFLLQVQSMGLLND 851

human: 600 HSMAQTLQASLEGLPPSTSSGQPPLQDMLCLGGVAVSLSHIRN* 642
             |  ||||  |||||   |   ||  |||||||||  ||  |||
mouse: 852 QHMTQTLQSSLEGLCSRTFPAQPLFQDMLCLGGVSVSQAHIRG* 894
```

Fig. 2 Comparison of amino acid sequences between human (upper sequence) and mouse MEI1 (lower sequence). There is 77% amino acid identity between the two sequences. *Vertical lines* Identical amino acids, *asterisks* stop codons

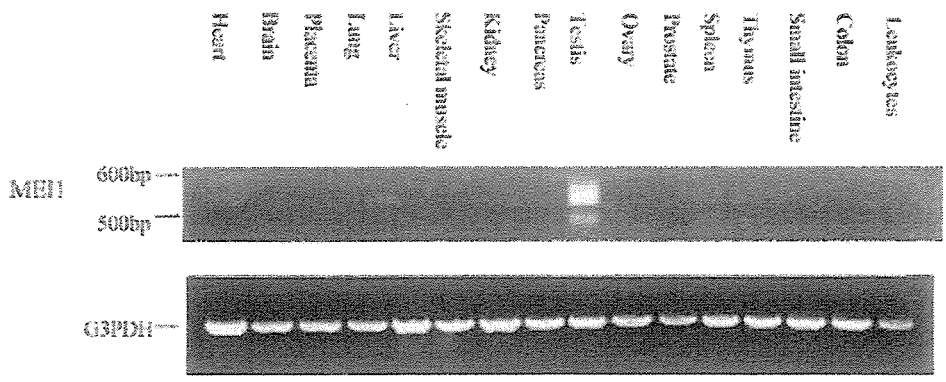

Fig. 3 RT–PCR analysis of human *MEI1* cDNA using primers EXP2F1 and EXP2R6. Expression patterns of *MEI1* in 15 human adult tissue cDNA samples were examined by PCR (*upper panel*). Two clear bands were detected in the testis and very weak bands were present in spleen and thymus. The upper and lower bands in the testis lane indicate the longer and shorter cDNAs, respectively. G3PDH was used as a positive control (*lower panel*)

Table 2 Genotype and allele frequencies of four coding single-nucleotide-polymorphism (cSNPs) in the human *MEI1* gene in 26 azoospermic patients (13 European Americans and 13 Israelis) and European American control individuals. *HWE* Hardy–Weinberg equilibrium

SNPs	Alterations		Genotype frequency					Allele frequency			
	Nucleotide	Amino acid	No of samples with genotype/total no of samples (%)			*P*-value[a]	HWE test[b]	No of chromosome with minor allele/total no of the chromosomes (%)			*P*-value[a]
			Genotype	Patients	Controls			Allele	Patients	Controls	
SNP1	909T/G	Synonymous	TG	15/26 (57.7)	16/53 (30.2)	0.0271*		G	17/52 (32.6)	40/106 (37.7)	0.4799
			GG	1/26 (3.8)	4/53 (7.5)	0.6622	0.37602				
SNP2	1582A/G	Thr/Ala	AG	1/26 (3.8)	0/56 (0)	0.3171	< 0.05	G	1/52 (1.9)	0/112 (0)	0.3171
SNP3	1791C/A	Synonymous	AC	4/26 (15.4)	0/60 (0)	0.0067*	0.33904	A	4/52 (7.7)	0/122 (0)	0.0073*
SNP4	2397C/T	Synonymous	TC	3/26 (11.5)	0/61 (0)	0.0245*	0.13582	T	3/52 (5.7)	0/122 (0)	0.0256*

*Statistically significant
[a]Fisher's exact test between patients and controls
[b]Genotypes significantly different from HWE proportions at $P = 0.05$ level

the respective zygosity in the two groups were 0.000/0.115/0.885 and 0.00/0.00/1.000 ($P = 0.0245$), and the allele frequencies were 0.057/0.943 and 0.000/1.000 ($P = 0.0256$). The most common genotypes for SNP3 and SNP4 in both groups were 1791C/C and 2397C/C. However, AC heterozygotes and TC heterozygotes were strikingly higher at the SNP3 and SNP4 sites in the patient group, respectively. There were no statistical differences for SNP1 and SNP2 in the two groups ($P > 0.05$ for both SNPs). Tests of HWE carried out for all SNPs among patients revealed that SNP2 of patients showed a significant deviation from HWE ($P < 0.05$).

We next analyzed a possible association of the *MEI1* SNPs with azoospermia separately among European Americans and among Israelis (Table 3). At the SNP3 site, the proportions of AA homozygote/AC heterozygote/CC homozygote in the 13 European American patients and their 61 controls were 0.00/0.154/0.846 and 0.000/0.000/1.000, respectively ($P = 0.0289$), and the frequencies for alleles A/C were 0.077/0.923 and 0.00/1.00, respectively, showing a significant difference ($P = 0.0299$). Similarly, at the SNP4 site, the proportions of the respective zygosity in the two groups were 0.000/0.154/0.846 and 0.000/0.000/1.000 ($P = 0.0289$), and the allele frequencies were 0.077/0.923 and 0.00/1.00 ($P = 0.0299$). However, no such association at the two polymorphic sites was observed between the 13 Israelis and their 60 control individuals ($P > 0.05$).

Haplotype analysis revealed that haplotype frequencies estimated for all four polymorphisms in the groups were close to each other, with no significant differences (data not shown). Haplotype estimation and LD analysis revealed different distributions of the haplotypes with SNP3 and SNP4 (Tables 4, 5). The SNP3–SNP4 (C–T), SNP3–SNP4 (A–C) and SNP3–SNP4 (A–T) haplotypes were revealed to be significantly more frequent in the European American patient group than in the European American control group. The SNP3–SNP4 (A–T) haplotype was also revealed to be significantly more frequent in the Israeli patient group than in the Israeli control group.

Discussion

We have isolated the human *MEI1* cDNA, which shares 61 and 77% homology at the nucleotide and amino acid levels, respectively, to the mouse *Mei1* cDNA. The

Table 3 Genotype and allele frequencies of SNPs 3 and 4 between 13 European American azoospermic patients and 61 controls, and between 13 Israeli patients and 60 controls

Populations	Genotype frequency				*P*-value[a]	Allele frequency			*P*-value[a]
	SNP	Genotype	No of samples with genotype/total no of samples (%)			Allele	No of chromosome with minor allele/total no of the chromosomes (%)		
			Patients	Controls			Patients	Controls	
Americans	SNP3	AC	2/13 (15.4)	0/61 (0)	0.0289*	A	2/26 (7.7)	0/122 (0)	0.0299*
	SNP4	TC	2/13 (15.4)	0/61 (0)	0.0289*	T	2/26 (7.7)	0/122 (0)	0.0299*
Israelis	SNP3	AC	2/13 (15.4)	1/60 (1.7)	0.0798	A	1/26 (3.8)	1/120 (8.3)	0.0819
	SNP4	TC	1/13 (7.7)	1/60 (1.7)	0.3265	T	1/26 (3.8)	1/120 (8.3)	0.3255

*Statistically significant
[a]Fisher's exact test between patients and controls